



Geochemical Characteristics And Their Implications On Origin Of Rajahmundry Trap Basalts Of Andhra Pradesh, India.

B. Ganesh¹, K. John Paul¹, A. A. Jaya Raj², Ch. Israel¹

1. Department of Geology, Acharya Nagarjuna University, Guntur, Andhra Pradesh, India.

2. Department of Civil Engineering University College of Engineering, Acharya Nagarjuna University, Guntur, Andhra Pradesh, India.

Abstract: Continental flood basalts are massive volcanic eruptions that accumulate enormous volumes of basaltic rock covering large areas in the order of lacks of square kilometers and attaining thickness of several hundreds of meters and volumes exceeding one million Km³. Rajahmundry Trap Basalt flows are one among such worldwide large continental flood basalts. For the last half a century, it has been an interested topic of research on CFBs for several geoscientists who have contributed voluminous data on basalts. In the present paper an attempt has been made to unearth the probable mode of origin and emplacement of RTB flows that are occurring as discrete out crops at several locations. 28 basalt samples were collected from three basalt flows one lying one the other separated by two intertrappeans and an infratrappean bed at the base of these flows. The samples were analyzed chemically by HR-ICP Mass Spectrophotometer for major, minor and trace elements and by XRD powder pattern. Initially these samples were studied under microscope in thin sections for mineral identification. These basalts are very fine grained with occasional phenocrysts of Olivine, Plagioclase and Clinopyroxenes and fine granules of these and many other minerals admixed with cryptocrystalline and glassy matrix. From the data derived from, optical, XRD and analytical procedures appropriate conclusions have been drawn.

Key Words: Geochemical, Trap Basalt flows, Intertrappeans, major and minor elements, trace and rare-earth elements, Differentiation, Crust, Mantle

INTRODUCTION

Basalts are extensive and spectacular rock formations in the earth's crust, both in Oceanic and continental environment. They are common rock types in volcanic regions. These rocks are melanocratic, fine grained and of high density. The term 'Basalt' was first introduced by Pliny, which signifies a black iron – bearing stone. Later the word Basalt was applied as a specific name is petrography by Agricola. But in recent times the word modern usage basalt may basalt is defined as mafic lava consisting of plagioclase feldspar and a group of mafic minerals in roughly equal proportions. The mafic or dark minerals consist mainly of Augite, Olivine, iron Oxides, apatite along with Hornblende, Hypersthene and Biotite, and the felsic minerals consisting of plagioclases ranging from Albite to Anorthite and there may be insignificant amounts of K–feldspar, Quartz, and glassy matrix. The term basalt is considered now as the simple mixture – Labradorite, Augite and iron oxides. The term "Olivine basalt" is used when olivine is present in significant amounts. Basalts are most commonly exhibiting a vesicular structure due to gas babbles or vesicle that are trapped during the solidification of lava. These bubbles after escape of gases can give basalt a porous appearance.

STUDY AREA

As per the Geological time scale the Rajahmundry Trap Flows (RTF) are considered to be of late cretaceous to early tertiary age. These Basalt flows of the Krishana – Godavari Basin are extended ~50km² on east and west sides of the Godavari River in Andhra Pradesh (Baksi et.al., 1994; Baksi, 2001; Sen and Sabale, 2011). It was considered by some authors that RTB are the eastward continuation of Deccan Traps thus representing an example of long-distance lava transport spreading over 1500km across India and about 70km into the Bay of Bengal (Jay 2005; Jay and Widdowson, 2008; Keller et al. 2008; Self et al, (2008). These basalts are striking NESW direction, with a dip of 5° to the SE towards the Bay of Bengal. Rajahmundry lava flows have a typical and well-established stratigraphic sequence generally underlain by late limestones, cretaceous age and overlain by the sandstone of Eocene age. The average thickness of exposed Rajahmundry lava flows is 60m including two intervening continuous sedimentary layers of lime stone, shale and red bole (~2m thickness) and an overlying lateralized basalt as in some areas like Pangidi, Gowripatnam, Duddukuru, Lakshmipuram and Kateru. The three lava flows are separated by red gravel soil and lime marl intratrappean, with fossiliferous layers (Fig.1&2). These two sedimentary intratrappeans separating the lower traps from the middle traps and middle traps from upper traps, indicates a break or periods of non-deposition of unknown duration before each lava flow emplacement. Flows are compositionally almost similar and are having holocrystalline, to mesocrystalline texture, light black in colour with phenocrysts of olivine, Albite, Anorthite, pyroxene embedded in ground mass of these minerals and glassy matrix and also other accessory minerals, like Ilmenite, Magnetite, Quartz, Orthoclase and secondary minerals Hematite and Goethite, as studied by many authors.



Fig. No.1: Field photograph of three basalt lava flows observed in thadimalla puntha quarry at Duddukuru.



Fig. No.2: Field photograph of three basalt lava flows observed in Pangidi quarry at Rajahmundry Trap Basalts.

GEOLOGY OF THE AREA

The RTB are considered as part of the Godavari Triple Junction. This particular region specifically preserves an excellent stratigraphic record of Mesoproterozoic to Neogene period providing evidence for Gondwana continental break-up period in Cretaceous and drifting (Lakshminarayana, 1996, 2002; Lakshminarayana et al., 2010). A sequence of mounds trending NE-SW between Rajahmundry, Gowripatnam and Duddukuru, covering an area of nearly 100 km², is represented as the RTB in the Krishna-Godavari Basin. The K-G Basin has been developed during Phanerozoic due to uplift of the basement that resulted in buildup of Eastern Ghats Mobile Belt. According to Lakshminarayana (1995a) a sequence of step faults oriented in NE - SW are the main cause for the development of major basins in the east coast since Mesozoic period. These blocks are identified as the Mailaram high, Raghavapuram Basin Dammapeta Basin, and Pangidi-Rajahmundry Basin extending from west to east. The Mailaram high was uplifted initially during early Mesozoic controlling the sedimentary sequence in the Dammapeta Basin. Later the Mailaram high became a watershed zone due to post Jurassic uplift, resulting in the development of small deltaic streams that flow towards east for the first time (Lakshminarayana, 1997). Outcrops of RTB are exposed in certain areas, such as Nallajerla, Decharla, Lakshmipuram, Bandapuram, Duddukuru, Gowripatnam, Pangidi, Kateru, Konthamuru and Rajahmundry with intervening sedimentary beds (GSI, 1996). But the prominent outcrops are exposed in five areas namely Pangidi, Gowripatnam, Duddukuru, Lakshmipuram and Kateru quarries. These discrete Rajahmundry Trap flows identified in separate areas are considered as a single unit (Lakshminarayana, 1995b). Those separate areas expose coastal Gondwana sediments of the east coast (Cretaceous), RTBs (K-Pg boundary), Rajahmundry sandstone Formations (Paleogene) and the recent sediments in the K-G Basin. The topmost horizon of the Tirupati Formation, forms the basement of the Rajahmundry Traps which is known as the 'Infratrappean beds' represented by limestone, sandstone and clay (Lakshminarayana et al., 1992). In the NW margin, the RTBs are bounded by a NE-SW fault, and are overlain by the Rajahmundry sandstone and Quaternary sediments towards east. The traps are also traversed by NW-SE faults at Duddukuru and Pangidi area. The complete and full stratigraphic sequence of RTBs is preserved in between, these two fault zones. The present investigation is mainly focussed on the prominent geological succession of Rajahmundry Traps from the Gowripatnam (17°01'37"N, 81°37'22"E), Duddukuru (17°01'57"N, 81°36'05"E) Pangidi (17°00'52" N 81°38'39"E), Lakshmipuram (17°00'49" N 81°35'06"E) and Kateru (17°03'06" N 81°47'33"E) quarry cuttings, located west and East side of the Godavari River. The RTB units here consist of three separate and distinct basaltic lava flows - lower, middle and upper intervened by two Intertrappean sedimentary layers which are described as Intertrappean I and II. The 15 to 30 m thick lower basalt flow is unconformably overlaying the (Maastrichtian-Danian) Infratrappean bed (Fig.1). Some physical volcanic features like rootless cones, and dyke like forms are noticed associated with the lower basalt flow along with multi-tier radial jointing and columnar structures. Intertrappean I consisting of 2.0 - 3.0 m thick, limestone, marl and clay intercalations is sandwiched in between lower and middle basalt flows of RTB. Many invertebrate fossils were identified from this limestone layer at Pangidi, Kateru, Gowripatnam, Duddukuru, Lakshmipuram, Dhecharla, Bandapuram and this fossil evidence has drawn great attention due the similarities with the sedimentary Intertrappeans of central and western India (Lakshminarayana et al., 2010; Malarkodi et al., 2010). The middle flow which is 5 - 10m thick, greenish grey vesicular basalt overlies unconformably the Intertrappean I. The upper flow overlies Intertrappean II which is made of red clay or red bole. The upper flow of 5 - 15 m thick unconformably overlying the Intertrappean II is vesicular fine-grained basalt.

Age	System	Formation	Lithology
Recent to Sub – Recent		Alluvium	Gravel, Sand, Silt, Clay and laterite.
Mio – Pliocene		Rajahmundry	Sandstone
-----Unconformity-----			
Upper Cretaceous t Lower Eocene	K /T boundary	Rajahmundry	Upper Trap (Basalt Rock) Intratrappian – II (Red clay or red bole) Middle Trap (Basalt Rock) Intratrappian -I (Lime layer) Lower Trap (Basalt Rock) Infratrappian Fossiliferous layer
Lower Cretaceous to Lower Triassic	Upper Gondwana	Thirupathi	Sandstones and Shale/ Clay
		Raghava Puram	Sandstones and Shale/ Clay
		Gollapalli	Sandstones and Shale/ Clay
	Lower Gondwana	Chintalapudi	Sandstones and Shale/ Clay
-----Unconformity----- ---			
Archaen			Khondalites, Charnokites and Gneisses

Fig. No.3: Showing Geological Succession of the study area after Manikyamba et.al. (2015) and central Ground water report (2016-2017).

SAMPLE COLLECTION AND LABORATORY PROCEDURES

Well exposed outcrops of basalt flows are identified on eastern and western side of Godavari River extending to a distance of approximately 60km around Rajahmundry. Samples of basalts were collected where quarrying is being carried out and stratigraphic sequence is prominently exposed. Some of the prominent quarry cuttings are 1) Sri Sivagowri Quarry at Duddukuru 2) Balaji quarry at Pangidi 3) Kondagudem quarry at Gowripatnam 4) Shesha Sai quarry at Lakshmipuram, all lining on the western side of Godavari River and 5) Cherukuri quarry at Kateru on the Eastern side of the Godavari River. There are also sporadic other places where RTB are exposed as small hills are mounds, but quarrying is not carried out. At all the quarrying places stratigraphic sequence exhibits three basalt flows one over the other and separated by two intratrappians and an Infratrappian at the base of lower flow and also a supertrappian on the top of the upper basalt flow. This sequence of three basalt flows with alternating sedimentary layers is considered as the boundary between cretaceous and Eocene ages (K-T boundary). At each location representative samples of required size (~10cm) were collected from each layer of basalt flow and labelled with serial number and preserved carefully in polyethene bags which again labelled with location and serial number, and carried to the laboratory for further analysis. About 45 samples were collected from all the locations and representative samples were later subjected to various analytical techniques.

Some field photographs have also been taken for description of super position of stratigraphic layers of basalt flows and other features like colour, texture, and vesicles and Amygdales and total elevation of cross -section of stratigraphic columns.

Various methods that are adopted for any investigation primarily dependent on the data required for the objectives set forth and availability of analytical techniques. Since the objectives of the present study on Rajahmundry Trap Basalts is to bring out certain geochemical characteristics and their interrelationships, some advance technical and Laboratory investigations both non-destructive and destructive methods are carried out.

The widely used laboratory techniques of mineral identification are; optical mineralogy, X-ray diffraction, modal analysis and Norm calculation, and XRF analysis for major, minor, trace elements, and rare-earth elements. Initially thin sections of basalts have been prepared and examined under advanced petrological microscope for mineral identification and calculation of modal mineral percentages carried out for representative samples. Basalt samples were then ground to powder and fine fractions of – 250 mesh size were taken for analysing the minerals by X-ray diffractometer, and for determining major, minor and trace elements by using XRF method and also for determining rare-earth elements by using HR-ICP mass spectrometer. CIPW Norm was calculated for each rock sample by using the major and minor elements.

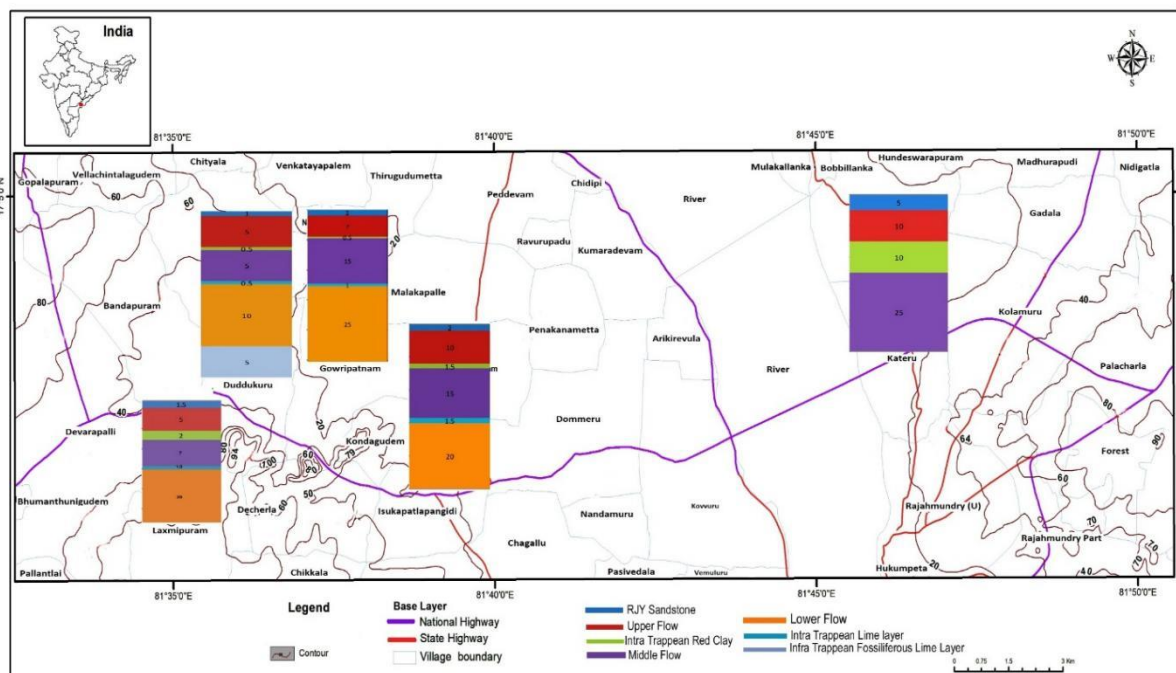


Figure No: 4. Showing Basalt flows and intratrappean layers with approximate thickness (in meters) at different quarry areas of Rajahmundry trap Basalts, and also, samples taken from each flow representing areas in map. The sample numbers are U1,U2,M1,M2,L1,L2 from Pangidi, and samle numbers U3,U4,M3,M4,L3,L4 are from Gowripatnam, the sample numbers U5,U6,M5,M6,L5,L6 are from Duddukuru, the samle numbers U7,U8,M7,M8,L7,L8 are from Lakshmiapuram and the sample numbers U9,U10,M9,M10 are from Kateru.

Area / Element	PGD						GPT					
	PU1	PU2	PM1	PM2	PL1	PL2	GU3	GU4	GM3	GM4	GL3	GL4
w%												
SiO ₂	47.04	47.26	47.11	47.14	47.05	46.93	47.21	47.89	47.04	47.39	47.03	47.18
Al ₂ O ₃	12.44	13.04	12.16	12.74	14.21	14.07	13.11	14.46	12.77	13.91	14.21	14.58
Fe ₂ O ₃	1.35	1.34	1.21	1.24	1.22	1.11	1.32	1.35	1.23	1.37	1.12	1.21
FeO	12.08	12.00	10.87	11.13	10.92	9.97	11.75	12.12	11.01	12.45	10.02	10.82
MnO	0.12	0.12	0.15	0.15	0.12	0.11	0.11	0.12	0.13	0.13	0.12	0.12
MgO	7.72	6.96	7.12	7.30	7.27	7.22	7.20	6.49	7.34	6.34	7.25	6.52
CaO	8.34	8.49	8.38	9.29	9.18	8.87	8.16	8.67	9.03	7.01	9.47	9.56
Na ₂ O	2.79	3.04	2.70	2.55	2.85	2.54	2.89	2.77	2.73	3.11	2.68	2.61
K ₂ O	0.09	0.11	0.16	0.17	0.08	0.06	0.10	0.13	0.08	0.26	0.09	0.07
TiO ₂	2.26	2.03	1.79	1.86	1.89	1.88	2.03	1.87	1.82	1.95	1.80	1.91
P ₂ O ₅	0.06	0.08	0.07	0.07	0.06	0.05	0.09	0.08	0.06	0.06	0.05	0.05
CO ₂	0.85	0.82	0.83	0.84	0.81	0.81	0.85	0.84	0.84	0.85	0.84	0.82
Cr ₂ O ₃	0.03	0.02	0.05	0.03	0.04	0.05	0.03	0.04	0.02	0.03	0.03	0.02
ZrO ₂	0.01	0.03	0.03	0.04	0.05	0.03	0.02	0.02	0.02	0.03	0.01	0.02
S	0.01	0.02	0.03	0.01	0.03	0.01	0.02	0.03	0.01	0.02	0.02	0.01
LOI	5.48	5.01	8.45	6.29	5.05	7.19	5.63	3.28	6.79	5.82	6.31	4.99
Total	100.67	100.37	101.11	100.85	100.83	100.9	100.52	100.16	100.92	100.73	101.05	100.49

Table No.1A: Major and Minor Elements laboratory analysis data of Pangidi (PGD), Gowripatnam (GPT) areas samples.

Area/Element	DDU						LKMP					
	DU5	DU6	DM5	DM6	DL5	DL6	LU7	LU8	LM7	LM8	LL7	LL8
w%												
SiO ₂	47.43	47.20	47.41	47.85	46.95	47.21	47.63	47.24	47.10	47.05	47.10	47.11
Al ₂ O ₃	14.24	14.40	13.92	13.62	12.78	14.96	13.35	14.40	12.19	12.79	13.41	14.07
Fe ₂ O ₃	1.34	1.33	1.39	1.41	2.24	1.19	1.53	1.35	1.20	1.25	1.27	1.25
FeO	12.05	12.17	12.47	13.91	9.35	10.70	13.75	12.11	10.80	11.03	11.37	11.21
MnO	0.12	0.11	0.12	0.11	0.12	0.14	0.13	0.13	0.13	0.12	0.13	0.12
MgO	6.60	6.75	6.37	6.51	7.72	6.72	6.31	6.75	7.11	7.31	7.21	6.90
CaO	7.38	7.29	7.07	6.99	8.48	10.20	5.71	7.26	8.32	9.02	9.28	8.60
Na ₂ O	3.01	3.10	3.00	3.09	2.73	2.73	3.17	3.10	2.66	2.72	2.74	2.55
K ₂ O	0.21	0.23	0.28	0.44	0.07	0.07	0.46	0.19	0.15	0.07	0.08	0.17
TiO ₂	2.33	1.41	1.97	2.11	1.86	1.94	2.05	1.33	1.77	1.80	1.88	1.64
P ₂ O ₅	0.09	0.11	0.08	0.13	0.06	0.07	0.11	0.09	0.05	0.07	0.07	0.06
CO ₂	0.81	0.81	0.82	0.83	0.82	0.81	0.82	0.84	0.84	0.81	0.83	0.82
Cr ₂ O ₃	0.01	0.02	0.01	0.04	0.03	0.02	0.01	0.02	0.03	0.03	0.03	0.01
ZrO ₂	0.01	0.01	0.03	0.02	0.01	0.02	0.03	0.01	0.02	0.02	0.03	0.02
S	0.02	0.03	0.02	0.03	0.03	0.02	0.04	0.01	0.04	0.03	0.02	0.03
LOI	5.14	5.55	5.04	3.25	6.76	3.38	5.32	5.74	8.57	6.77	5.47	6.16
Total	100.79	100.52	100.00	100.34	100.01	100.18	100.42	100.57	100.98	100.89	100.92	100.72

Table No.1B: Major and Minor Elements laboratory analysis data of Duddukuru(DDU), Lakshmipuram (LKMP) areas samples.

Area / Element	KATERU			
	KU9	KU10	KM9	KM10
w%				
SiO ₂	47.22	47.14	48.06	46.25
Al ₂ O ₃	14.41	13.74	11.80	12.74
Fe ₂ O ₃	1.35	1.22	2.72	1.33
FeO	12.19	10.97	10.04	11.21
MnO	0.13	0.12	0.23	0.12
MgO	6.76	6.77	2.71	8.30
CaO	7.32	8.44	10.88	7.29
Na ₂ O	3.12	2.56	2.12	1.55
K ₂ O	0.20	0.08	0.54	0.37
TiO ₂	1.39	1.89	3.55	1.86
P ₂ O ₅	0.10	0.06	0.20	0.06
CO ₂	0.84	0.82	0.80	0.79
Cr ₂ O ₃	0.01	0.02	0.04	0.02
ZrO ₂	0.01	0.02	0.02	0.01
S	0.02	0.03	0.03	0.03
LOI	5.42	6.44	7.25	8.29
Total	100.49	100.32	100.99	100.22

Table No.1C: Major and Minor Elements laboratory analysis data of Kateru area samples.

Area / Elements	PGD						GPT					
	PU1	PU2	PM1	PM2	PL1	PL2	GU3	GU4	GM3	GM4	GL3	GL4
Li(7)	5.987	7.588	6.156	5.673	4.979	5.126	5.087	5.771	5.580	6.876	5.140	4.730
V(51)	331.535	338.275	338.342	369.032	256.571	251.456	335.142	338.040	362.672	324.489	286.604	310.051
Cr(53)	169.012	159.818	107.476	119.408	135.249	129.236	133.874	72.506	159.204	63.125	159.674	172.006
Co(59)	51.756	48.946	51.619	48.532	41.878	43.277	51.944	48.141	49.273	51.024	40.891	39.488
Ni(60)	113.084	101.487	92.520	87.289	91.967	102.265	110.828	72.984	101.735	75.215	88.407	79.257
Cu(63)	197.274	212.430	222.663	193.160	145.526	146.639	201.010	448.482	190.614	209.965	146.451	151.558
Zn(66)	199.952	147.602	348.871	142.284	189.770	375.553	184.616	145.384	221.730	94.013	368.452	281.964
Ga(71)	21.755	22.097	19.775	20.506	17.590	17.408	21.840	22.823	21.539	21.786	17.783	18.295
Rb(85)	1.231	1.549	3.681	3.450	1.563	1.474	1.322	4.109	1.173	3.966	1.403	1.329
Sr(88)	263.194	277.304	290.103	274.051	241.476	234.966	291.394	276.014	287.411	282.014	233.829	243.684
Zr(90)	137.115	150.763	137.467	135.502	97.021	96.327	141.367	192.771	125.213	180.125	97.913	103.702
Nb(93)	12.390	13.208	9.391	9.762	6.544	6.183	12.428	13.720	8.889	11.413	6.261	6.360
Mo(95)	0.742	0.918	0.700	0.973	0.613	0.522	0.757	1.017	0.709	0.860	0.560	0.591
Ba(137)	52.010	69.981	350.159	157.540	53.187	74.679	58.817	197.415	53.407	104.246	51.507	44.248
Hf(178)	3.464	3.801	3.504	3.541	2.543	2.459	3.515	4.856	3.294	5.130	2.587	2.836
Ta(181)	0.917	0.934	0.611	1.170	0.511	0.498	1.401	0.995	0.692	1.049	0.485	0.523
Pb(208)	0.752	0.700	1.119	0.813	1.354	1.589	0.801	0.963	0.928	0.833	2.354	1.705
Th(232)	1.200	1.335	1.302	1.331	1.031	0.882	1.213	1.951	1.075	1.966	0.899	0.913
U(238)	0.338	0.381	0.603	0.487	0.216	0.263	0.362	0.450	0.300	0.633	0.242	0.194

Table No.2A: Trace elements analysis data of Pangidi (PGD) and Gowripatnam (GPT) area samples.

Area / Erea	DDU						LKMP					
	DU5	DU6	DM5	DM6	DL5	DL6	LU7	LU8	LM7	LM8	LL7	LL8
Li(7)	6.965	8.959	6.404	4.676	4.699	8.855	8.365	7.257	6.780	4.553	4.602	4.602
V(51)	429.639	322.549	324.489	260.554	370.381	227.215	225.432	350.363	370.237	326.704	329.667	329.667
Cr(53)	65.023	63.255	64.752	116.731	208.234	37.458	37.162	108.446	162.459	156.734	152.212	152.212
Co(59)	49.046	49.246	50.678	43.554	46.860	44.478	44.478	54.125	50.266	51.520	52.414	52.414
Ni(60)	74.527	73.215	75.185	98.598	95.954	54.542	53.879	93.459	108.633	117.566	118.450	118.450
Cu(63)	288.097	299.255	209.784	151.024	163.416	556.846	556.340	220.255	190.746	175.355	171.659	171.659
Zn(66)	157.186	109.452	94.135	288.325	129.044	226.874	226.289	350.448	225.215	110.604	97.870	97.870
Ga(71)	23.388	21.146	21.810	16.978	20.945	22.546	24.416	19.459	23.255	20.962	20.626	20.626
Rb(85)	2.109	2.635	3.822	1.416	0.825	10.236	9.718	4.124	1.590	1.150	1.090	1.090
Sr(88)	285.670	279.257	281.936	245.532	278.776	276.479	276.607	295.125	289.855	287.424	286.169	286.169
Zr(90)	182.705	175.479	179.532	94.263	107.733	355.215	350.110	137.467	128.237	109.606	108.438	108.438
Nb(93)	13.197	12.569	11.855	6.402	6.964	24.125	23.328	9.391	9.854	7.148	7.403	7.403
Mo(95)	0.953	2.146	0.862	0.774	0.665	1.965	1.739	0.732	0.259	0.608	0.652	0.652
Ba(137)	127.316	179.479	104.752	41.709	48.277	452.475	440.774	350.159	54.257	76.290	64.257	64.257
Hf(178)	4.645	5.510	4.675	2.435	2.955	8.077	8.077	4.013	3.898	2.850	2.827	2.827
Ta(181)	1.138	1.126	0.958	0.457	0.569	1.936	1.685	0.933	1.025	0.488	0.652	0.228
Pb(208)	0.966	0.833	0.748	0.674	0.585	1.969	1.406	1.562	1.585	0.753	0.577	0.652
Th(232)	1.784	1.523	1.854	0.806	0.906	4.257	3.403	1.124	1.235	0.908	0.867	0.577
U(238)	0.418	0.914	0.410	0.227	0.234	0.937	0.825	0.426	0.755	0.232	0.228	0.867

Table No.2B: Trace elements analysis data of Duddukuru (DDU) and Lakshmipuram (LKMP) area samples.

Area / Element	KATERU			
	KU9	KU10	KM9	KM10
Li(7)	8.485	8.854	4.983	6.743
V(51)	321.927	321.998	326.704	368.132
Cr(53)	62.075	62.746	157.652	117.418
Co(59)	48.059	48.146	50.500	47.532
Ni(60)	71.057	71.246	115.566	87.289
Cu(63)	295.760	295.958	176.355	192.130
Zn(66)	109.353	109.452	111.604	141.284
Ga(71)	21.986	21.146	20.962	21.506
Rb(85)	1.761	2.585	1.190	2.450
Sr(88)	272.581	272.987	288.324	273.151
Zr(90)	169.845	170.143	109.606	133.502
Nb(93)	11.412	11.255	7.148	9.962
Mo(95)	1.088	1.875	0.608	0.863
Ba(137)	152.029	178.146	76.290	158.640
Hf(178)	4.337	5.246	1.950	3.641
Pb(208)	0.834	0.965	0.863	0.913
Th(232)	1.676	1.846	1.918	1.831
U(238)	0.382	0.846	0.352	0.399
Ta(181)	0.873	1.025	0.588	0.970

Table No.2C: Trace elements analysis data of Kateru area samples

Area / Element	PGD						GPT					
	PU1	PU2	PM1	PM2	PL1	PL2	GU3	GU4	GM3	GM4	GL3	GL4
Sc(45)	32.350	32.513	32.352	34.135	25.960	25.052	30.343	35.443	33.662	36.451	29.264	31.382
Cs(133)	0.050	0.049	0.091	0.078	0.077	0.061	0.047	0.065	0.052	0.099	0.052	0.046
La(139)	10.664	11.914	10.314	10.640	6.858	6.587	10.323	15.573	9.092	15.125	6.831	7.146
Ce(140)	25.919	28.898	24.827	25.793	17.266	16.744	25.394	37.597	22.852	36.325	17.591	18.332
Pr(141)	3.627	4.052	3.497	3.648	2.541	2.429	3.592	5.185	3.293	4.758	2.577	2.688
Nd(146)	17.332	19.451	16.886	17.669	12.597	11.991	17.317	24.466	16.287	22.449	12.876	13.444
Sm(147)	4.725	5.258	4.629	4.855	3.606	3.402	4.754	6.450	4.638	5.882	3.692	3.930
Eu(153)	1.587	1.758	1.541	1.627	1.285	1.236	1.631	2.007	1.596	1.255	1.327	1.391
Gd(157)	5.234	5.814	5.237	5.483	4.219	3.966	5.282	7.086	5.297	7.458	4.335	4.605
Tb(159)	0.836	0.929	0.849	0.894	0.656	0.613	0.853	1.141	0.855	1.533	0.674	0.714
Dy(163)	5.058	5.579	5.204	5.449	4.080	3.862	5.183	6.949	5.160	6.585	4.207	4.469
Ho(165)	1.040	1.158	1.094	1.152	0.838	0.782	1.063	1.453	1.082	1.286	0.861	0.910
Er(166)	2.651	2.912	2.816	2.945	2.159	2.024	2.698	3.737	2.716	3.215	2.194	2.336
Tm(169)	0.368	0.403	0.398	0.413	0.296	0.276	0.375	0.527	0.375	0.785	0.299	0.318
Yb(172)	2.375	2.600	2.602	2.685	1.903	1.770	2.428	3.435	2.422	3.125	1.911	2.032
Lu(175)	0.332	0.363	0.368	0.378	0.264	0.245	0.340	0.485	0.338	0.965	0.264	0.280

Table No.3A: REE elements laboratory analysis data of Pangidi (PGD) and Gowripatnam (GPT) area samples.

Area / Erea	DDU						LKMP					
	DU5	DU6	DM5	DM6	DL5	DL6	LU7	LU8	LM7	LM8	LL7	LL8
Sc(45)	38.103	37.012	35.951	23.958	37.996	30.254	30.094	33.013	34.585	31.729	31.631	31.631
Cs(133)	0.046	0.864	0.099	0.055	0.039	0.245	0.123	0.237	0.895	0.048	0.043	24.630
La(139)	14.244	15.245	14.314	6.369	7.371	26.166	26.166	10.314	9.102	7.306	7.210	0.043
Ce(140)	34.276	35.458	34.654	15.972	18.959	63.670	63.670	24.827	22.852	18.590	18.255	7.210
Pr(141)	4.718	7.257	4.899	2.312	2.803	9.236	8.722	3.497	4.257	2.725	2.684	18.255
Nd(146)	22.266	24.786	22.476	11.493	14.075	45.125	40.763	16.886	17.457	13.598	13.399	2.684
Sm(147)	5.905	8.125	5.999	3.251	4.174	11.459	10.543	4.629	5.125	3.891	3.869	13.399
Eu(153)	1.903	2.190	1.901	1.138	1.483	3.322	3.035	1.541	1.626	1.372	1.378	3.869
Gd(157)	6.475	9.246	6.421	3.751	4.843	12.458	11.385	6.014	5.713	4.484	4.428	1.378
Tb(159)	1.046	3.547	1.005	0.605	0.795	1.458	1.800	0.215	1.025	0.737	0.725	4.428
Dy(163)	6.395	7.125	5.458	3.711	4.778	11.785	10.971	6.015	6.325	4.401	4.379	0.725
Ho(165)	1.351	3.013	1.113	0.769	0.993	3.255	2.309	1.965	1.965	0.912	0.905	4.379
Er(166)	3.489	3.345	3.152	1.941	2.501	7.257	5.928	2.546	2.759	2.295	2.290	0.905
Tm(169)	0.496	0.722	0.529	0.271	0.344	1.255	0.835	0.966	0.585	0.319	0.318	2.290
Yb(172)	3.248	4.246	2.986	1.759	2.214	5.257	5.438	2.895	2.549	2.064	2.052	0.318
Lu(175)	0.460	1.025	0.404	0.459	0.247	0.308	0.964	0.767	0.125	0.257	0.289	2.052

Table No.3B: REE elements laboratory analysis data of Duddukuru (DDU) and Lakshmipuram (LKMP) area samples.

Area / Elements	KATERU			
	KU10	KU11	KM9	KM10
Sc(45)	36.006	36.115	31.760	34.562
Cs(133)	0.049	0.146	0.048	0.088
La(139)	13.550	13.146	7.306	9.640
Ce(140)	32.660	32.479	18.590	24.793
Pr(141)	4.515	5.413	2.725	3.648
Nd(146)	21.263	21.549	14.598	15.569
Sm(147)	5.634	6.857	3.991	4.935
Eu(153)	1.844	1.954	1.422	1.259
Gd(157)	6.224	8.575	4.484	6.483
Tb(159)	1.005	2.146	0.817	0.994
Dy(163)	6.189	6.986	4.601	7.449
Ho(165)	1.291	2.588	0.952	2.152
Er(166)	3.325	3.245	2.315	2.126
Tm(169)	0.471	0.585	0.449	0.413
Yb(172)	3.079	4.126	2.174	2.685
Lu(175)	0.436	0.936	0.349	0.378

Table No.3C: REE elements laboratory analysis data of Kateru area samples.

Mineralogy

To have clear understanding on the genetic aspects of any rock, it is essential to have insight into its material characteristics like mineral constituents, their textural or interlocking patterns or the fabric and the geochemical elements present and their relative proportions. Order of crystallisation of minerals from the parent magma from which rocks solidify is also essential to know the genetic history of the rock. The minerals identified in Rajahmundry Trap Basalts (RTBs) by various laboratory and Instrumental methods are classified into three categories 1) Essential and 2) Accessory. Albite, Anorthite, Diopside, Augite, Hypersthene, Forsterite and Fayalite, constitute the essential minerals, and Magnetite, Ilmenite, Apatite, Cristobalite, Stishovite, and Quartz constitute the accessory minerals. The secondary minerals like Kaolinite, Montmorillonite, Goethite and Hematite, which are the alteration products of primary minerals and also some cryptocrystalline and amorphous material has been identified in glassy Metrix. Various methods like optical, XRD, normative, Modal and physical characteristics, were employed for the identification and confirmation the minerals.

GEOCHEMISTRY

Chemical analyses of important fresh and semi- weathered basalts collected from different quarry cuttings at Pangidi, Gowripatnam, Duddukuru, Lakshmipuram and Kateru where stratigraphic sequences are well exposed, have been carried out and are presented in table Numbers 1A,1B and 1C for major and minor elements, 2A,2B and 2C for trace elements and 3A,3B and 3C for rare earth elements. A systematic and comparative study was carried out by collecting basalt samples from each location by picking up from three flows of basalts to bring out geochemical, mineralogical and textural differences among them.

Major Elements:

From the chemical analysis of basalts, it is evident that there is no considerable difference in the major elements weight percentages when compared among three basalt flows.

The silica SiO_2 content ranging from 47.05 - 48.06 wt.%, and a moderate to high ranges of MgO 2.71-8.30wt% and CaO 5.71 – 10.88 wt.% Table and Al_2O_3 content showing a narrow range between 11.80 and 14.63 wt.% (1A,1B & 1C), distinctly depict the tholeiitic character. The rocks are typically enriched in iron with 9.35 - 13.91 wt.% FeO . As K_2O content ranges from 0.06 - 0.54 wt.% and in terms of SiO_2 vs K_2O , the RTBs are considered as low-K sub-alkaline tholeiites RTBs have TiO_2 content ranges from 1.33 - 3.55 wt.%. Na_2O content ranging from 1.55 – 3.17w% and CO_2 also present ranging from 0.79 – 0.85w%.

Minor and Trace Elements:

All rocks contain trace elements in low concentration usually less than 0.1 % by wight. Therefore, the concentrations are commonly expressed in (ppm) parts per million or (ppb) parts per billion. The minor elements are analysed by advanced techniques using X-ray Fluorescence spectroscope (XRF) and pyrometry and High Resolution Inductively Coupled Plasma – Mass Spectrometry (HR-ICP-MS). Minor elements analysed in basalt samples of the study area include elements like Strontium (Sr), Barium (Ba), Rubidium (Rb), Chromium (Cr), Zirconium (Zr), Nickel (Ni), Niobium (Nb), Scandium (Sc), and Vanadium (V). The elements potassium (K), Phosphorous (P) are considered as major elements. However, their low concentrations in rocks like basalts are also to be considered as trace elements as they play a significant role in petrographic studies. Zirconium (Zr), and Niobium (Nb) are important for understanding the petrogenesis of igneous rocks in distinguishing between different magma types, such as tholeiitic and alkaline basalts. Nickel (Ni) and chromium (Cr) trend to be concentrated in mafic and ultra mafic rocks.

Trace elements are widely used as testing models of magmatic differentiation. In this process the proportions, of trace elements that remain in the liquid are calculated after certain mineral is separated by fractionation. This testing can also be utilised to estimate the degree of partial melting required to generate a particular magma. Therefore, the method is a testing model of partial melting and fractional crystallisation.

Trace elements present in different types of primary magmas indicate depths in the mantle the at which the magmas are generated at different. At very shallower depths the mantle is consisting of plagioclase - lherzolite, at depths ranging between 40 and 80 km it consists of spinel - lherzolite, whereas at depths > 80 km it consisted of the garnet lherzolite. Plagioclase consists of strontium in the structure, spinel concentrates V+ Cr in crystal structure. And garnet concentrates HREE in its crystals structure respectively. So, magmas that are produced by small degree of melting at shallower, depths will be depleted in strontium. Those magmas from moderate depths will be depleted in V and Cr and those from > 80km will be depleted in HREE. So, in this way lherzolite plays crucial role in understanding the mantle processes as it is the major source of basaltic magma. The probability of acceptance of a trace element various mineral lattices depend primarily on its ionic radius and charge and it also depends on the crystal field effects and electronegativity of the element. According to

the element characteristics a trace element will either replace a major element in the crystal structure of the mineral or remains in the liquid. Trace elements analyses data of Rajahmundry Trap Basalts occurring in different locations are provided in the table Nos. (2A,2B & 2C).

Geochemical Relationships between Major and Minor Elements:

The fate of an elements during crystallization of magma mainly depends on the concentration of the element in the magma and the nature of the lattice structures that may form. The silicon and aluminium concentration and the temperature of the magma are the controlling factors in the sequence of crystal lattice formations. The crystal lattices thus formed act as a sorting mechanism for the cations in the magma. A cation of similar size can enter a crystal lattice with appropriate coordination number. In general, numerous different ions have to satisfy this requirement. The ion which is present in largest amount holds its position in the lattice with greatest tenacity. From the study of crystal structures and energy considerations, Goldschmidt (1954) was able to formulate the following empirical rules that can be used as a general guide to the course of an element during liquid → crystal formation in a multicomponent system:

1. When two trace elements have the same radius and charge, they will incorporate into a given mineral lattice with equal opportunity.
2. when two trace elements have dissimilar radii and same charge, then the smaller one can enter more readily into crystal lattice of a mineral.
3. When two trace elements have same radii and different charges, the one with higher charge will more readily enter the crystal lattice of a mineral.

Goldschmidt's rules are of greatest utility in the predicting of the order of removal of the major elements as well as of the minor elements from a magma.

Minor Elements in Magmatic Crystallization: When a minor element has the similar charge and ionic radius as the major element, then it is said to be *camouflaged* in the crystal lattice contain that the major element. When a minor element has same ionic radius but a higher charge than that of a major element, then the minor element is *Captured* by that crystal lattice which contains the major element. When a minor element has a same ionic radius and a lower charge than that of a major element it is then said to be *admitted* into the crystal structure that contains the major element.

Gallium:

Gallium with the similar ionic radius and charge very close to that of aluminium is camouflaged in aluminium bearing minerals. Though the size of gallium ion (Ga^{+3} , $62A^\circ$) is somewhat larger than aluminium ion (Al^{+3} , $51A^\circ$) it suggests that gallium would be more abundant in later formed aluminium minerals (Fig No.5). Ga: Al ratio in igneous rocks show that the ratio is almost constant, indicating that gallium is effectively camouflaged in aluminium minerals, but with little tendency in later differentiations. Concentration of Ga ranges from 15.578 to 20.962ppm in lower layer of basalt, 19.459 to 23.255ppm in middle layer and 21.146 to 24.416ppm in the upper layer of basalt flows.

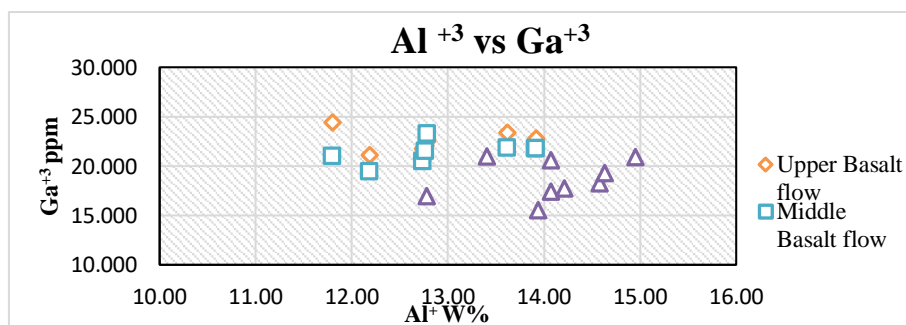


Fig. No. 5. Graph Showing Al^{+3} vs Ga^{+3} with Al:Ga almost constant in three layers in basalts.

Hafnium:

Hafnium with the same charge and radius (Hf^{+4}) ($0.78A^\circ$) as that of Zirconium (Zr^{+4} , $0.79A^\circ$) always occurs camouflaged in Zirconium minerals. Hence a constant ratio Zr: Hf remains throughout the process of

fractional crystallisation. The figure 6 shows a fairly positive correlation between Zirconium and Hafnium in three layers of trap Basalts. The concentration ranges of Hafnium are 2.335ppm to 2.955ppm in lower, 2.335ppm to 5.130ppm in middle and 1.950ppm to 8.077ppm in upper layer. Zirconium does not enter into combination of rock forming minerals to any degree, but appears in a distinct phase as Zircon. Zircon is most abundant in later differentiation processes in residual magmatic solutions. Both zirconium and Hafnium are also associated with Ilmenite substituting the Titanium in the Ilmenite lattice structure.

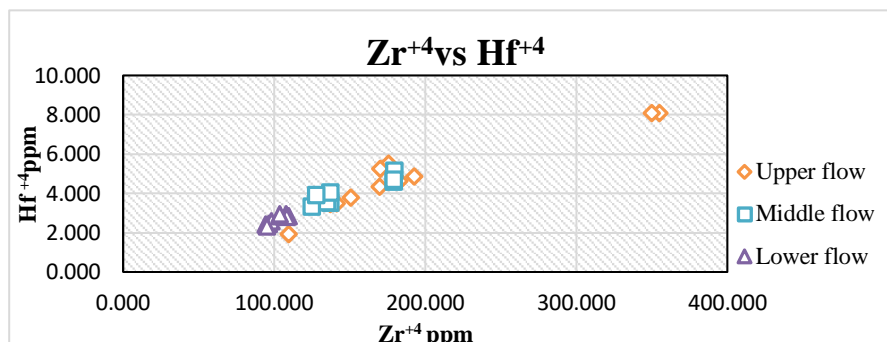


Fig. No. 6. Shows Zr^{+4} vs Hf^{+4} with constant Zr: Hf ration in three layers of basalts.

Cobalt (Co^{+2}):

Cobalt is present in all Igneous rocks in the form of Co^{+2} ($0.72A^\circ$) ion substituting Fe^{+2} . Because of ionic charge Co^{+2} is camouflaged in ferrous compounds ($0.72A^\circ$). But however, it is formed that the ratio Co: Fe is grate in early formed minerals and decreasing steadily with increasing fractionation. The effective radius of Cobalt is somewhat less than radius giving above and appaerly almost identical with that of Mg ($0.66A^\circ$). The major part of the cobalt in a magma is removed in the early formed magnesium minerals, especially olivine. The figure (7) shows a fairly increasing and decreasing correlation between ferrous iron and cobalt. The concentrations range of cobalt are 39.398 ppm to 52.414 ppm in lower layer, 48.532ppm to 54.125ppm in middle layer and 44.478ppm to 52.068 ppm in the upper layer of basalt flows.

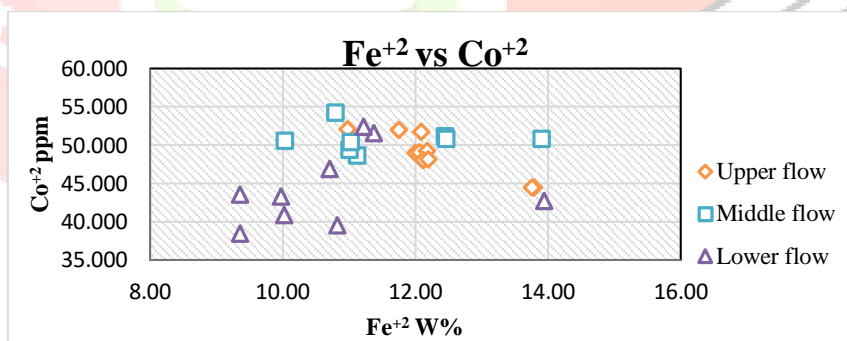


Fig. No. 7. Showing Fe+2 Vs Co+2 with Fe: Co ratio increasing and decreasing trends in the three layers of basalt flows.

Nickel:

Nickel ion (Ni^{+2}) has same radius ($0.69A^\circ$) and some charge as that of magnesium ion (Mg^{+2}) ($0.66A^\circ$). Having same charge and radius, it is expected to be camouflaged in Mg – minerals. However, the ratio Ni: Mg is high in early crystallised minerals like Olivine and there is a steady decline in later formed rocks and minerals. The Rajahmundry trap basalts clearly show fairly positive correlation (Fig:8) between Ni and Mg in the lower, Middle and upper layers. The range of Ni Concertation are 78.257ppm to 118.450ppm in lower layer, 75.177ppm to 115.566ppm in middle layer and 71.057ppm to 120.694ppm in upper layer of basalt flows.

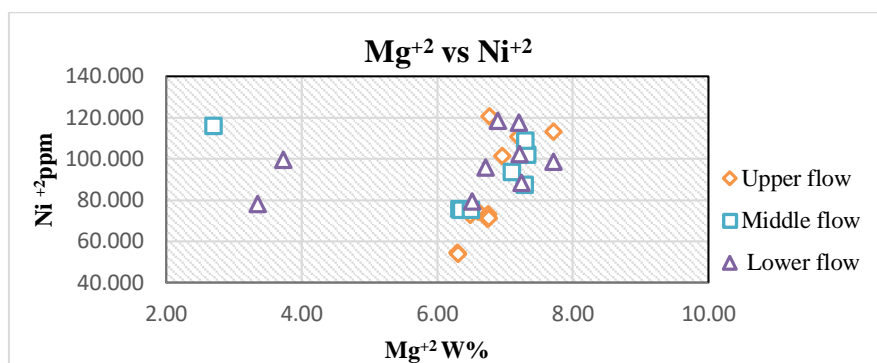


Fig. No. 8. Graph showing Mg^{+2} vs Ni^{+2} with fairly positive correlation in the three layers of basalts.

Manganese (Mn):

Manganese is present in magmas as Mn^{+2} ($0.80A^\circ$) ion and in this form, it is expected to proxy for Fe^{+2} ($0.74A^\circ$) or for Ca^{+2} ($0.99A^\circ$). However, manganese is much more electronegative than calcium and probably on this account rarely found replacing the element. The manganese in the igneous rocks replace ferrous iron and the relative increase in the Mn: Fe has been noted in later differentiation indicating that somewhat larger size of the manganese ion causes it to be admitted in ferromagnesian minerals. Manganese is absent in calcium – bearing plagioclase. The figure (9) shows fairly possible correlation between Fe^{+2} and Mn^{+2} in three layers of basalts. The concentration ranges are 0.11 to 0.14w% in lower layer 0.11 to 0.23w% in middle layer and 0.11 to 0.13w% in upper layer.

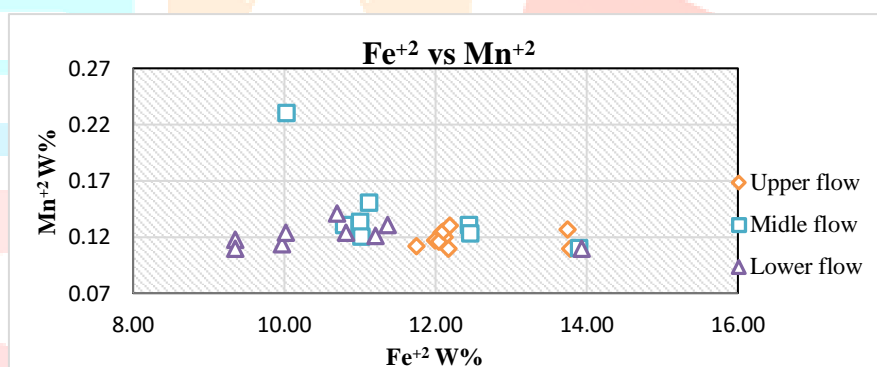


Fig. No. 9. Graph showing Fe^{+2} vs Mn^{+2} with fairly possible correlation between Fe^{+2} and Mn^{+2} .

Vanadium:

Vanadium is present in magmas as V^{+3} ($50.95A^\circ$). It is removed from magma largely in magnetite in which it proxies for Fe^{+3} . Its ionic radius is slightly larger than Ferric iron ($0.64A^\circ$) and its electronegativity is much less for which reason there is enrichment of Vanadium in early formed magnetites. Vanadium also occurs in the structure of pyroxenes, Amphiboles and Biotite. It shows marked concentration in Aegirine, a mineral of high Fe^{+3} . Fig. No.10 shows that V^{+3} has partial positive correlation with Fe^{+3} as in the case of Chromium ion. The concentration ranges are 251.456 - 370.381ppm in lower layer 324.489ppm to 370.237ppm in middle layer and 225.432 - 429.639ppm in upper layer.

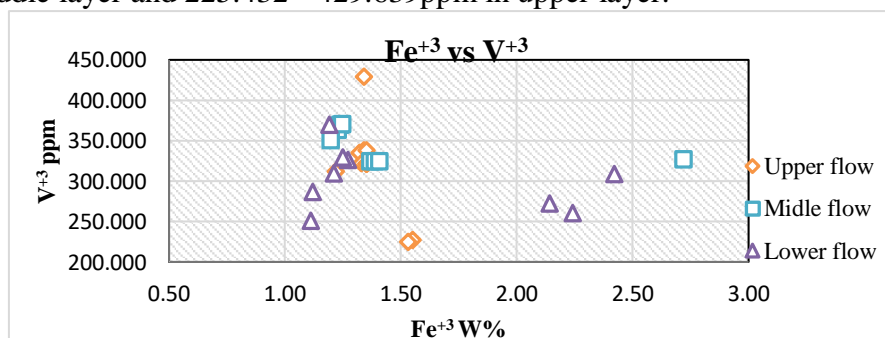


Fig. No. 10. Graph shows Fe^{+3} vs V^{+3} in the partially positive correlation between the two ions.

Chromium:

Chromium is present in magmas as Cr^{+3} ions. The radius of chromium ion (0.63\AA) is close to that of Fe^{+3} (0.64\AA). Having high degree of preferential relation to ferric ion, it is removed in the early stage of crystallisation as chromite mineral. This is due to smaller electronegativity of Cr^{+3} compared to that of Fe^{+3} . Chromium ion is enriched in pyroxenes of basic rocks in the later stage of crystallisation. The graph between Fe^{+3} vs Cr^{+3} (Fig. 11) shows that chromium concentration decreases at constant rate with Ferric ion with the fall of temperature during magma crystallisation. Positive correlation is observed in three basaltic layers. The concentration ranges of Chromium are 116.731- 208.234ppm in lower layer, 63.125 - 162.459ppm in middle layer and 37.162 - 169.012ppm in upper layer.

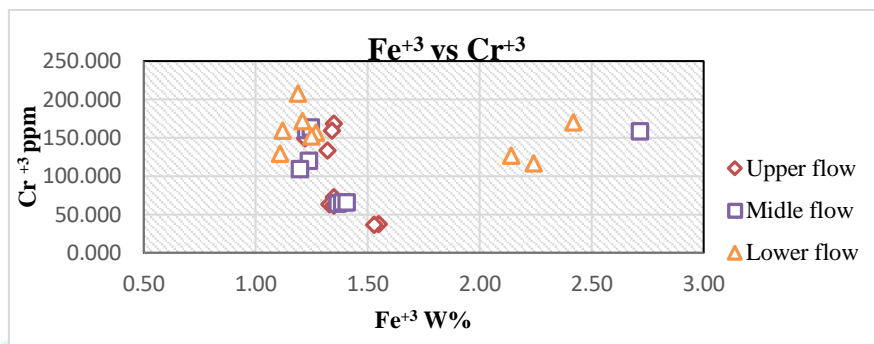


Fig. No. 11. The graph between Cr^{+3} vs Fe^{+3} shows that Cr^{+3} and Fe^{+3} are with positive Correlation in three layers of basalts.

Titanium:

Titanium (Ti^{+4}) is present in igneous rocks mainly as Ilmenite. It substitutes Al^{+3} in six – coordination and appears in pyroxenes, Hornblende and biotite. Ti^{+4} is captured by such minerals because of its higher charge. Titanium shows (Fig.12) partially positive correlation with aluminium in three Basalt layers. The concentration ranges of Titanium are 1.64 - 2.94w% in lower layer, 1.82-3.55w% in middle layer and 1.33-2.26w% in upper layer. In highly siliceous magmas titanium occurs as Titanite CaTiSiO_5 .

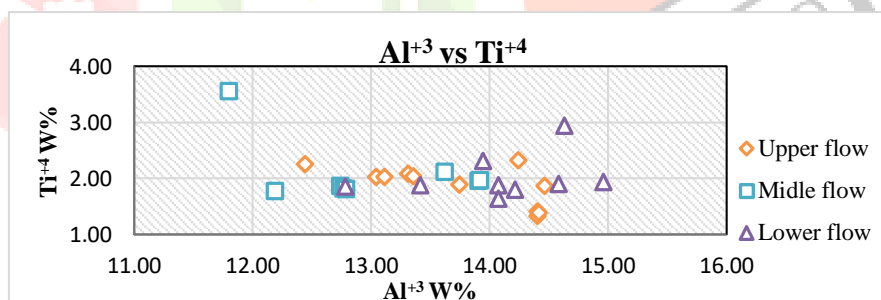


Fig. No. 12. Graph showing Al^{+3} Vs Ti^{+4} with partially positive correlation, in middle, upper and lower basalt layers.

Lithium:

On the basis of chemical properties, lithium follows the other alkali elements in magmatic processes However ionic size is decisive factor during crystallisation. Lithium ion (Li^{+} : 0.68\AA) is very much smaller than any of alkali ions (Na^{+} : 0.97\AA : K^{+} : 1.33\AA) Hence Lithium follows magnesium since ionic sizes are almost identical (Mg^{+2} , 0.66\AA). Because of its lower charge, lithium ion is admitted into magnesium minerals. The Li: Mg ratio shows a steady increase in later formed rocks and minerals. Li: Mg ratio can be used as an index to the stage of differentiation (Strock). Lithium is found in pyroxene, Amphiboles and particularly in micas. The concentration ranges of Lithium are 4.553-5.140ppm in lower layer, 4.983-7.257ppm in middle layer and 5.087-8.959ppm in upper layer. Very partial positive correlation is observed between Li and Magnesium (Fig.13) in trap basalts of Rajahmundry in the three layers.

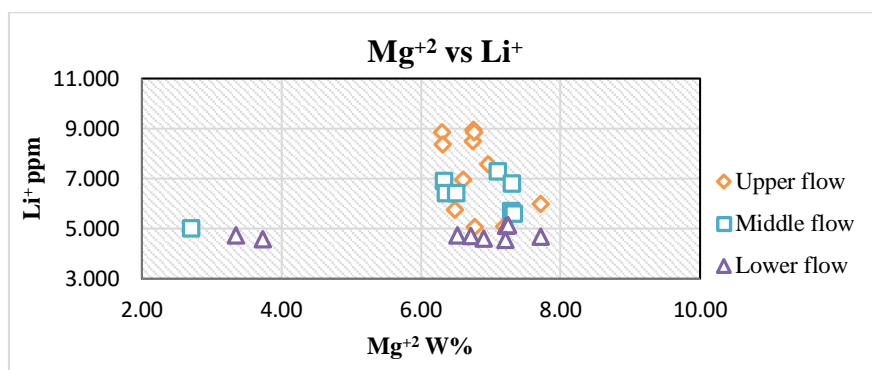


Fig. No. 13. Graph showing the Very patrial positive correlation between Li and Magnesium in the three layers of basalt flows.

Strontium:

The size of strontium Sr^{+2} (1.12 \AA) is such that it can replace either calcium (0.99 \AA) or Potassium (1.33 \AA). Being higher in radius strontium in admitted into Calcium minerals and having higher charge captured by potassium minerals. Available data indicates that the strontium in Basalts is present in plagioclase and potash feldspars. Concentration of Sr increases as crystallisation proceeds. Positive correlation implies admittance is the dominant process in removing the strontium from basaltic magma since plagioclase are dominant feldspar minerals. Insignificant strontium is present in augite, since structure of pyroxenes does not readily accommodate it. Strontium shows considerably positive correlation with calcium in all the three Basalt layers. The concentration ranges of strontium are 233.829-287.424ppm in lower flow, 274.051-290.103ppm in middle flow and 272.987-291.394ppm in upper flow.

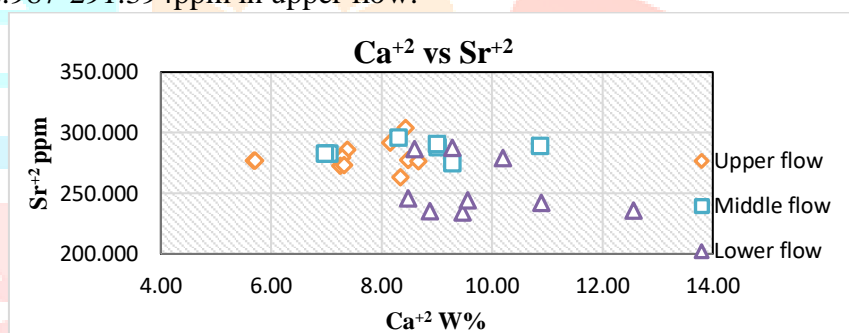


Fig. No.14. The Strontium showing considerably positive correlation with calcium in all the three Basalt layers.

Lead:

Lead is present in trace elements in many igneous rocks. It is present as Pb^{+2} (1.20 \AA) ion substituting K^{+} . Because of its higher ionic charge, Pb^{+2} is captured in to potassium minerals; but this tendency is wreaked by much electronegativity of Pb^{+2} . Hence lead in admitted rather than captured by potassium minerals. There is almost no correction of Pb^{+2} with K^{+} in lower basalt layer, but moderate correlation exists in middle and upper layer. Concentration ranges of lead are 0.577-1.905ppm in lower layer, 0.732-1.585ppm in middle layer and 0.637-1.969ppm in upper layer.

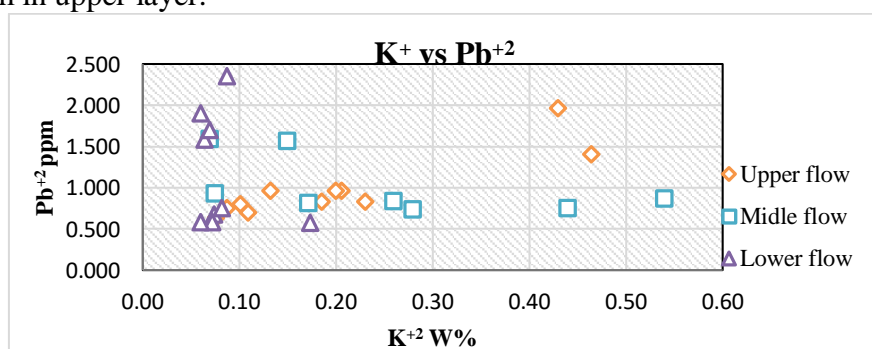


Fig. No. 15. Graph showing K^{+} vs Pb^{+2} with the moderate correlation between them.

Barium:

Barium ion is very large (1.34 \AA) in size to replace either Ca (0.99 \AA) or K (0.97 \AA). Hence, the major element comparable in ionic size is potassium. And therefore, Barium appears in Biotite and potash feldspar. Because of its higher charge Ba^{+2} ion is captured by potassium minerals due to their early crystallisation from magma. The Basalts of study area shows very much less concentrations of Ba^{+2} in Lower Basalts flow compared to middle and upper flows in which Ba^{+2} shows positive correlation with K^+ . The barium concentration ranges from 41.709-76.290ppm in lower flow 53.407-350.159ppm in middle flow and 47.847-452.475ppm in upper basalt flow.

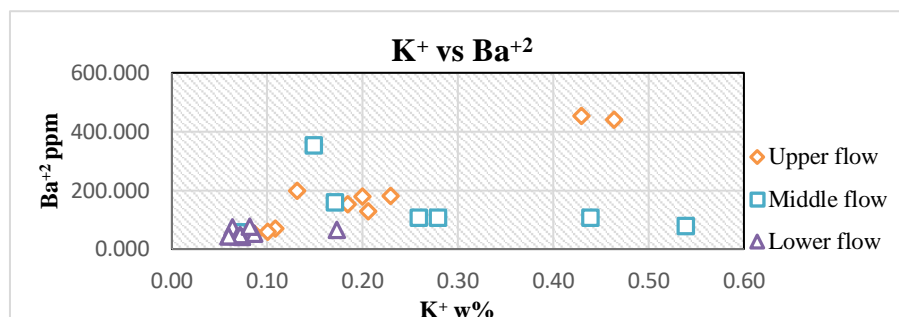


Fig. No. 16. The graph showing Ba^{+2} Vs K^+ with positive correlation between them in lower and upper basalt flows.

Rubidium:

Rubidium do not form mineral of its own. It is always incorporated into the structure of potassium minerals Biotite and potash feldspar, on account of its higher charge. Since Rb^{+2} (1.47 \AA) considerably larger than K^+ , rubidium is admitted into potassium minerals. Rb: K ratio increases with increasing differentiation as the magma cools and crystallises. Due to this reason Rubidium concentration reaches maximum in micas and K – feldspar. Rubidium concentration is very much less in lower Basalt flows compared to middle and upper flows in which there is moderately positive correlation between Rubidium and potassium. Concentration ranges of rubidium are 0.825-1.563ppm in lower flow 1.173-4.1247ppm in middle flow and 1.211- 10.236ppm in upper basalt flow.

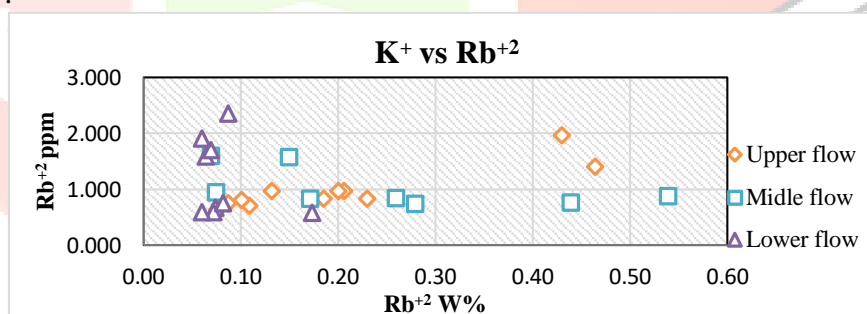


Fig. No.17. Graph shows moderately positive correlation between Rubidium and potassium in the middle and upper basalts flows.

Rare Earth Elements:

Th 17 metallic elements including lanthanides (atomic numbers from 57 to 71) and the elements Scandium (Sc, atomic number 21) and Yttrium (Y, atomic number 39) are grouped rare – earth elements. These elements, are not actually concentrated in the earth's crust, but they are dispersed and difficult to extract and purify. They are essential components of high-tech applications and are vital for technologies like smart phones, electric vehicles, renewable energy, automobile energy, medical applications, defence applications etc. The demand for REEs is increasing due to their importance in the transition to a green economy and technological advancements. The Rare Earth Elements (REEs) are divided into two sub groups-light and heavy rare earths. LREEs include Cerium (Ce), Lanthanum (La), Neodymium (Nd), Promethium (Pm), Praseodymium (Pr), Samarium (Sm), Gadolinium (Gd) and Europium (Eu), and HREEs include Dysprosium (Dy), Terbium (Tb), Holmium (Ho), Erbium (Er), Thulium (Tm), Ytterbium (Yb), Lutetium (Lu), scandium (Sc) and Yttrium (Y).

Among all the LREE and HREE only Lanthanum (La) Cerium (Ce), Praseodymium (Pr), Neodymium (Nd) Gadolinium (Gd) scandium (Sc), Yttrium(Y), shows variation in concentrations in different sample of the three layers of basalts. but the remaining rare earth elements Samarium (Sm), Promethium (Pm), terbium (Tb), Europium (Eu), Dysprosium (Dy), Holmium (Ho), Erbium (Er), Thulium (Tm), Ytterbium (Yb), Lutetium (Lu), are showing constant and low concentrations in all the sample of the three layers of the basalts.

Majority of the REEs are metallic with metallic lustre, and they are known for their unique magnetic, luminescent and geochemical properties. Naturally REEs are found in the structures of about 200 minerals, but major sources include Bastnasite, Euxenite, Monazite, Xenotime, Zircon and Allanite.

Rare earths are found in Basalts and their abundance and distribution can provide insights into the origin and evaluation of Basaltic magmas. Basalts being a common volcanic rock can exhibit varying REE patterns depending on the source rock and melting processes. Basalts typically contain a range of REEs, including LREs and HREs. The relative abundance of REEs in basalt can be represented on chondritic – normalised diagrams revealing patterns that can be used to infer magmatic processes. Fractional crystallisation and partial melting are the two main key processes that influence the REE distribution pattern of basalts. Some basalt show enrichment in LREEs. While others exhibit depleted LREE patterns possibly indicating specific mantle sources.

Rare Earth elements mainly substitute the Calcium ions in trace in most of the calcium bearing minerals. The essential rare earth elements that are analysed in the Rajahmundry trap Basalts are furnished in the table Nos. (3A,3B &3C).

Geochemical Relation of Rare Earth Elements with Major Elements:

Higher charge and comparatively larger ionic radius of the rare earths (Lu 0.85\AA - La 1.14\AA) with their low concentration in igneous rocks, suggest that there is little tendency to substitute major elements during crystallisation of magma. It is because of this reason that rare earths crystallise as individual minerals. Some of the rare earths also replace Ca^{+2} in lattice structures of certain minerals like Apatite and Hornblende.

Lanthanum:

Lanthanum (La) is chemical element with atomic number 57, found in group 3 of periodic tables and belongs to lanthanide series, it is primarily found in minerals bastnaesite and Monazite. These minerals are not identified in the basalts of the study area hence Lanthanum can be expected to be lodged in the structures of the other silicate minerals like Biotite, Apatite, Pyroxene and Feldspars. Lanthanum being trivalent (La^{+3}) is admitted in to the large cations Ca^{+2} . There is a negative correlation between the concentrations of Lanthanum and calcium in the three basalt layers (Fig. 18). There is more enrichment of Lanthanum in middle and upper basalt layers. Concentration ranges of Lanthanum are 6.269-7.371ppm in lower layer and its concentration range in the middle layer is 7.306-15.126ppm and its concentration is 10.323 -26.166ppm in the upper layer of the basalt flows.

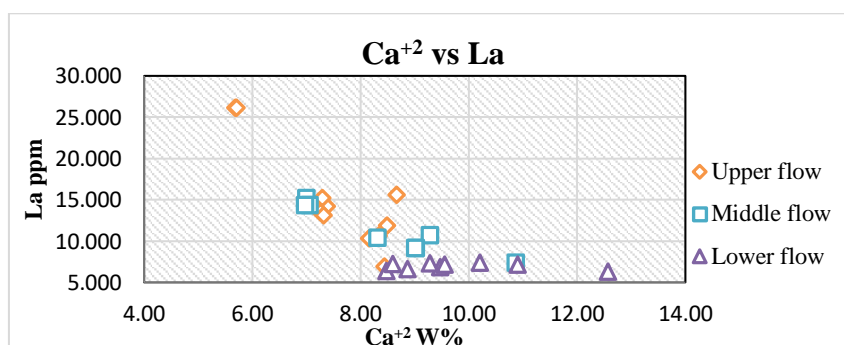


Fig. 18. Graph showing negative correlation between La^{+3} and Ca^{+2} for three layers of Basalts.

Cerium (Ce):

Cerium with atomic number 58 is a soft silvery metal. It is found in minerals like bastnaesite and Monazite but these minerals are not identified in the basalts of the study area. Hence it is expected that Cerium being large in size, substituting calcium bearing minerals like Biotite, Apatite, Pyroxene and Feldspars. Cerium being trivalent (Ce^{+3}) is admitted in to the large cations Ca^{+2} . There is a contrast between the concentrations of Cerium in the three basalt layers. There is more enrichment of Cerium in upper and lower basalt layers. The concentration ranges of the Cerium are 14.865-18.959ppm in lower layer and its concentration range in the middle layer is 18.590-36.325ppm and its concentration in the lower layer is 14.862-18.959ppm.

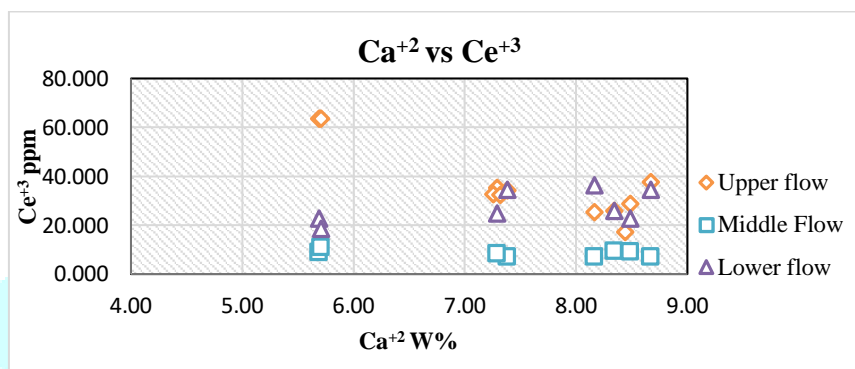


Fig. 19. Graph showing partially negative correlation between Ca^{+2} and Ce^{+3} for the upper and middle layers of basalts.

Praseodymium (Pr):

Praseodymium (Pr) is characterised by its presence in various minerals monazite, bastnaesite and Apatite. It is associated with other rare earths like cerium and lanthanum. Praseodymium is a trivalent ion (Pr^{+3}) and its geochemical behaviour is similar to other rare earth elements showing a tendency to be enriched in certain geological environments like calcium aluminium rich inclusions. Praseodymium is found normally in crystals and rocks with an abundance of 8.7 ppm by weight. Since the praseodymium bearing bastnaesite and monazite are not identified in the basalts of the study area it is expected to be present in the structures of hornblende and Apatite substituting Ca^{+2} . Concentration range of Praseodymium are 2.546- 9.236ppm in upper layer, and it is 2.725- 4.758ppm in the middle layer and it is 1.912- 2.803ppm in the lower layer. The general trend of the praseodymium in all the three layers is decreasing trend Fig: (20) its relative concentration decreases in all the three layers in later stages of differentiation of the magma, which indicates that larger size of the praseodymium (1.06 \AA) ion is admitted into Ca-Fe-Mg minerals.

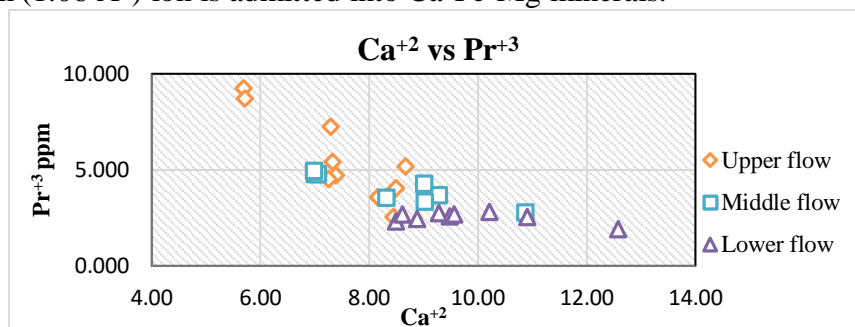


Fig: 20. Graphs shows Negative correlation between Ca^{+2} and Pr^{+3} in the three layers of Rajahmundry Trap Basalt.

Neodymium (Nd):

Neodymium (Nd) is a rare earth element especially silvery rare earth metal used for permanent Magnets, Neodymium is also larger trivalent cation (Nd^{+3} , 1.04\AA) which captured by Ca-Mg-Fe minerals like Hornblende substituting Ca^{+2} . Neodymium concentration range is 12.706ppm to 45.125ppm in upper layer, and its concentration is 14.598ppm to 22.476ppm in middle layer, and also its concentration range is 10.993ppm to 14.391ppm in Lower layer. Similar to the other rare earth elements concentration decreases in the later stages of differentiation process showing negative anomaly Fig: (21).

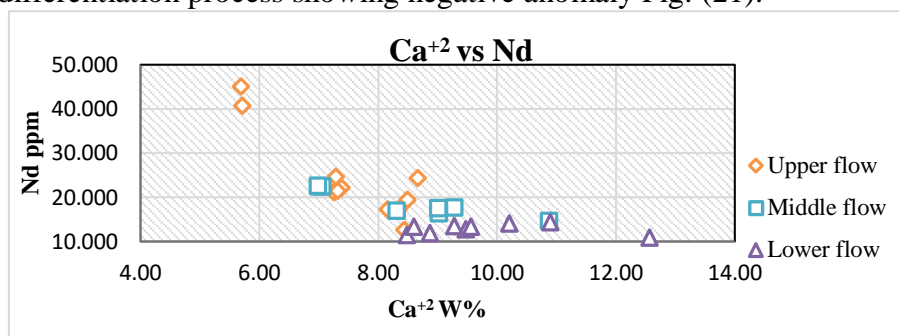


Fig: 21. Graph showing between Ca^{+2} vs Nd with negative correlation in three basalts layers at RTB.

Scandium (Sc):

Scandium with atomic number 21 has radius (Sc^{+3} , 0.81\AA) which is close to that of ferrous iron. But in view of its higher charge, Scandium is expected to be captured by ferromagnesium minerals. This is observed in magmatic pyroxenes which generally have a relative concentration of scandium. It may also present in Biotite and Hornblende. Scandium will not enter in the early formed Olivine because of the difficulty arising in balancing the positive charge followed by other suitable replacement. Scandium concentration in the basalt ranges from 30.094- 38.103ppm in upper layer and it is 31.760-36.451ppm in middle layer and it is 22.958- 37.996ppm in lower layer. Unlike the other rare earth elements, the concentration Partially decreases in the later differentiation process showing positive anomaly in three layers of basalts Fig: (22).

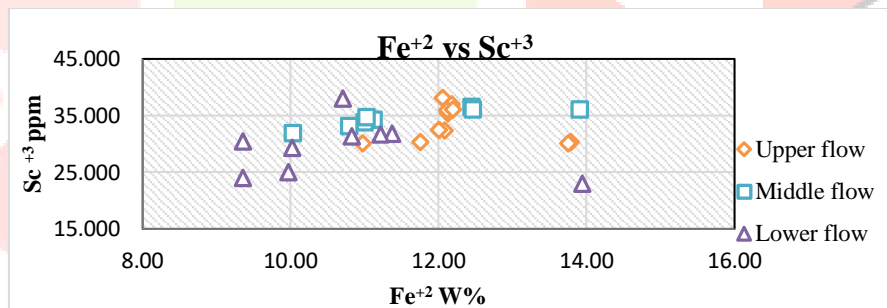


Fig. 22. Graph showing positive correlation between Sc^{+3} vs Fe^{+2} in the three basalt layers.

Yttrium (Y):

Yttrium (Y) is a trivalent chemical element atomic charge 0.92\AA a silvery-white, ductile transition mineral with atomic number 39. It is often classified as Rare Earth element due to its chemical similarity to the lanthanides Yttrium bearing minerals are primarily Xenotime which is an inclusion of Zircon, and also minerals Euxenite and Monazite. The inclusion present in the Zircon mineral contains various heavy mineral assemblies for distinguishing zircons for different sources. Yttrium concentration range in the basalt is 23.488- 65.245 ppm in Upper layer and it is 24.610- 33.933 ppm in Middle layer and it is 20.767- 26.696 ppm in Lower layer. Yttrium also shows decreasing trend with Ca in the latter stages of differentiation process during solidification of basalt lava.

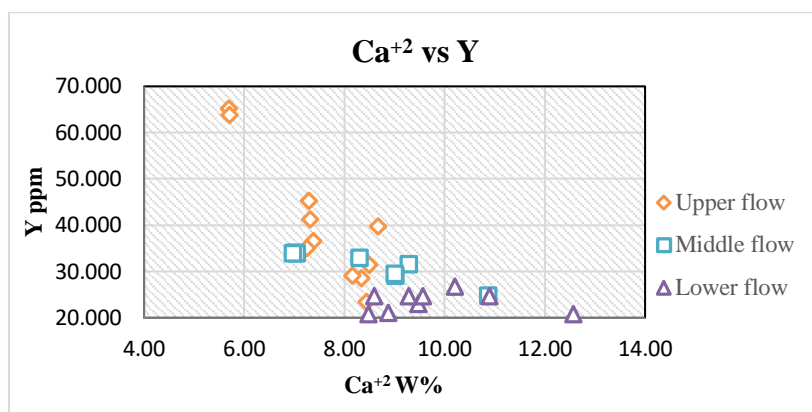


Fig. 23. Graph showing negative correlation between Ca^{+2} and Y, in three layers of basalt formations at RTB.

Gadolinium (Gd):

Gadolinium (Gd) exhibits unique geochemical properties. It is difficult and a classified as refractory lithophile element. In most igneous systems Gd is incompatible in mineral melt partitioning which means it concentrates in the liquid-phase during magmatic process. Generally, Gd has low fluid rock partition coefficients indicating its incompatible nature. Gadolinium also exists as a trivalent ion (Gd^{3+}) similar to other rare earth elements. Since gadolinium bearing minerals are not identified in the basalts it is presumed to be present in the Hornblende crystal's structure substituting the Ca^{+2} . Concentration range of Gadolinium are 4.246-12.458ppm in upper layer and it is 4.484-7.458ppm in the middle layer and its concertation 3.751-5.605ppm in lower layer. Similar to rare earths Cerium, Lanthanum, Praseodymium, it also shows decreasing trend towards later stages of differentiation as the basalt lava solidifies.

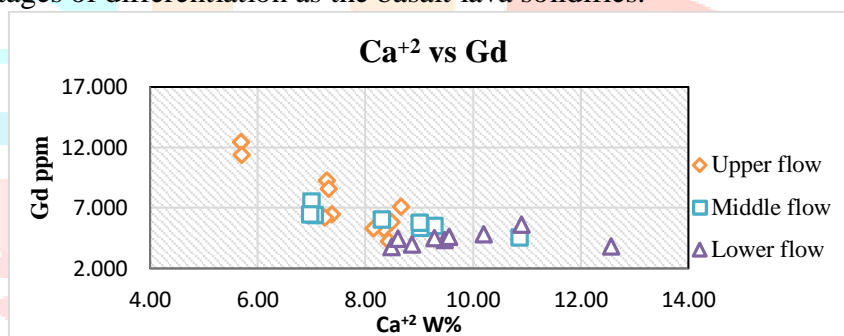


Fig: 24. Graph showing the correlation between Gd^{+3} and Ca^{+2} with decreasing trend.

DISCUSSION

Geochemical Interpretation:

Abundance of literature has evolved in recent years on basalts since these basalts are occurring on various locations of the earth's crust including continental regions, ocean floors as mid Oceanic ridges, as oceanic Islands and as Island arcs with different geological ages different way of formations and erupted in different climatic conditions and in different geographical locations. The geochemistry of basalts powerful tool for determining tectonic setting understanding mantle processes and practical application of carbon sequent ratio.

Key geochemical indicators major elements like silica (SiO_2), Iron (FeO_t), Magnesium (MgO) Calcium (CaO) and Aluminium (Al_2O_3) as well as trace and rare earth elements (REEs) and Isotope Ratios (Ex: Sr, Nd and Pb). The geochemical signatures such as Nb/ La and negative niobium anomalies help in differentiating between basalts from different tectonic environments like Mid Oceanic Ridges (MORB), Oceanic Islands (OIB), Island arcs and continental settings. Variation in the contents of major elements can also indicate the degree of partial melting and fractional crystallization in the magma evolution. The concentrations of trace elements including incompatible elements and REEs are sensitive to magma source and processes like assimilation and fractional crystallization. For instance, enrichment in light rare earth elements (LREE) as compared with Heavy Rare Earth Elements (HREE) is common.

To understand the geochemical nature of the basalts occurring in various regions of the world it is customary to compare the geochemical elemental data with that of the average chemical composition of undifferentiated

earth's mantle in the beginning. Standard values of the earth's primitive mantle are published by different earth scientists. For comparing the chemical data of the study area, the standards given by Sun and McDonough (1989) has been made use for further interpretation of the values. Standard values earth's primitive mantle for major and trace elements are normalized to the Sun and McDonough. Standard values are used to interpret the elemental composition of rock. The primitive mantle normalized values are a standard way of expressing the relative abundance of trace elements in rocks dividing the contents of each element in the rock by the content in the primitive mantle. The values derived from the work of Sun and McDonough (1989) was updated in 1995. They have given the values of the primitive mantle trace and rare earth elements as Rb (0.6), Ba(16.42), Th(0.045), U(0.021), Nb(0.26), Ta(0.03), Ce(2.12), Sr (51.38), P (276), K (150), Nd (0.26), Zr (11.67), Hf (0.36), Pb (0.03), Sm(0.55), Eu(0.2), Ti(1199), Y(5.58), Yb(0.58), La(0.08), Gd(0.71), Tb(0.0519), Dy(0.87), Ho(0.567), Er(0.53), Tm(0.071) and Lu(0.9). The normalized values are then plotted on diagrams called "multi-element" or "spider" diagrams to compare the trace element patterns of different magmas and geological materials. Values equal to >1 indicates enrichment, while values <1 indicate depletion relative to the primitive mantle.

Rajahmundry trap Basalts are Mid – Titanium to High – Ti Quartz tholeiites with a distinct variety. Which indicates the evolution of magma through fractional crystallisation and generation from Fe rich mantle at depths of 60 to 100 km. These basalts show limited contamination as indicated by the high K_2O/P_2O_5 and low Nb/La ratios. The RTB are generated from the melting of a Fe rich mantle occurring at depths of 60 to 100 km as inferred from the chemical analyses of major elements. The RTB basalts show a range of silica (SiO_2) content from 47.03 to 48.06 wt.%, moderate to high contents of MgO and CaO (2.71 to 7.72 and 5.7 to 10.88 wt.% Table (1a,1b), and Al_2O_3 showing a marginal range between 11.80 and 14.96 wt.%. These ranges are distinct evidences of the tholeiitic character of these basalts. The basalts show typical enrichment in iron (Feo + Fe_2O_3) from 11.08 to 15.32 wt.%.

As K_2O is present in the ranges of 0.06 - 0.54 wt.% and in view of SiO_2 and K_2O ratio, the RTBs are considered as low-K sub-alkaline tholeiites. Since the TiO_2 content of RTB ranges from 1.33 to 3.55 wt.%, basing on TiO_2 %, these basalts are divided into two groups as mid-Titanium basalts ($TiO_2 \leq 2.0$ wt.%) and as high Titanium-basalts ($TiO_2 \geq 2.0$ wt.%) where 2 wt.% of TiO_2 is treated as the boundary for the compositional range of basalts related to plume origin occurring all over the world that have erupted in both the oceanic continental environments (Safonova, 2009; Simonov et al., 2014). According to this classification the mid-Ti basalts of the study area have TiO_2 ranging from 1.74 to 1.92 wt.%, while the high-Ti basalts have TiO_2 ranging from 2.03 to 2.81 wt.%. Differentiation Index (D.I.) is used as Geochemical parameter for estimating magmatic differentiation. The DI of RTB basalt shows (Thornton and Tuttle, 1960) a wide range of variations from 39 to 52 supports middle to late-stage differentiation (Cox, 1980; Wilson, 1989). The major elemental percentages of basalts of study area shows consistency with tholeiitic basalts of Deccan Traps and Ocean Island Basalts (OIB) (Hughes, 1982; Sun and McDonough, 1989).

CIPW norm mineral percentages showed the presence of quartz (0.87 to 10.134 wt.%) and hypersthene (2.7612 to 29.5096 wt.%). The silica-saturated, quartz tholeiitic character of these basalts can be inferred from the mineral percentage in norm. In the total alkalis ($Na_2O + K_2O$) and silica (SiO_2) diagram (Le Bas et al., 1986; Le Maitre, 2002), Fig. 35 the samples of study area fall within the field of basalt, distinct depicting a sub-alkaline composition of these RTBs. These basalts also exhibit a distinctly tholeiitic character in the AFM diagram (Fig.36) (after Irvine and Baragar, 1971). High contents of some major elements such as Fe_2O_3 , CaO, MgO, and TiO_2 indicate a negative relationship with increase of D.I. whereas Al_2O_3 , K_2O and Na_2O contents show a positive trend with D.I.

Trace elements substitution of major elements in crystals is governed by Goldschmidt's rules which states that successful substitution depends on similar ionic charge and ionic radius. Trace elements are normally present at very low concentrations typically < 0.1 % by weight. These trace elements are incorporated into, mineral structures by replacing major elements if their charge and ionic radius are comparable. This process requires maintaining electrical neutrality within the crystal lattice and is influenced by ionic potential, electro negativity and crystal field effects. Ionic charge and radius of trace elements are crucial factors to substitute the major elements. If the charge differs, the substitution must be accompanied by substitution of another element to maintain the overall charge balance of the crystal. The electronegativity of an element and its ionic potential (charge or radius ratio) also play a role in strongly bonding within the crystal structure. The concentration of the trace element in the surrounding fluid also influences the extent of its incorporation in to the mineral structure. Temperature and pressure conditions are also playing a role in the stability of crystal structure and the likelihood of substitution.

Because trace elements behave differently from major elements and are more sensitive to variations in the source of magma and differentiation history, they act as valuable "fingerprints" for Geologists. After

substitution by trace elements the composition of a mineral significantly altered, making it the richer source of that particular trace element. By the patrons of trace elements substitution earth scientists are able to know the processes that form igneous rocks, mantle evaluation and also planetary differentiation.

Rubidium (Rb), Barium (Ba) and Strontium (Sr) can substitute (either by capturing or admitting) for potassium (K) and calcium (Ca) in minerals like feldspars due to similar ionic radii and charges. Transition metals like Nickel (Ni) Chromium (Cr) Cobalt (Co) and Vanadium (V) can substitute (either by camouflage or by capture) for magnesium (Mg) and iron in the minerals like Olivin and pyroxene.

Rare - earth elements with their variable ionic radii, can substitute for elements like calcium (Ca) and potassium (K), so that their substitution is complex and highly dependent on the available crystal size and other trace element present. Rare earth elements based on their geochemical nature are divided in to two groups – compatible and incompatible. Compatible Rare - Earth Elements (REEs) refers to specific REEs being incorporated into crystal structure of specific minerals particularly heavy REEs in garnet and LREEs called incompatible are concentrated in the general magmatic melts. Though all 17 rare earth elements are often found together their compatibility varies based on factors like ionic size and specific mineral's crystal size characteristics. Rare Earth elements are generally divided into 1) Light rare Earth Elements (LREEs) 2) and Heavy Rare Earth Elements (HREEs). Under LREEs Lanthanum (La), Cerium (Ce), Praseodymium (Pr), Neodymium (Nd), Promethium (Pm), Samarium (Sm), and Europium (Eu) are included. Under HREEs Gadolinium (Gd), Terbium (Tb), Dysprosium (Dy) Holmium (Ho), Erbium (Er), Thulium (Tm), Ytterbium (Yb), and Lutetium (Lu) are included. Scandium (Sc) and Yttrium (Y) are often grouped with REEs since they occur in the same ores with similar chemical characters. Partition co-efficient relates to ionic size and how strongly an element partitions in the particular mineral or melt, with smoother relationship indicating greater compatibility. For this reason, HREEs are considered more compatible with certain minerals like Garnet making them associated with these minerals rather than in the surrounding molten materials. LREEs are generally considered incompatible with the commonly, early crystallised mafic minerals found in magmatic system. The concept of compatibility is crucial in geochemistry. Its helps in understanding the magma evolution and mineral formation.

Trace elements ratios refer significantly between basalts and the mantle source, because partial melting and magma ascent differentially concentrate certain elements leading to distinct geochemical signatures. Compatible elements of similar chemical behaviour and ionic radii (La/Sm, Th/Yb) often maintain the ratios through partial melting reflecting source characteristics, while ratios of incompatible elements like Nb/ U can vary significantly depending on the extent of melting and source depletion or enrichment. Hence these ratios act as useful tools for tracing magma evolution and magma genesis.

Rare Earth Elements ratios used for comparison between Mantle source and Basaltic Rocks are described with the following examples:

Lanthanum / samarium (La/Sm), the ratio of light to Heavy REEs can indicates depletion or enrichment in the source. A high La/sm (2.283) -as compared with the La/Sm of mantle indicates (0.82/0.55) that the source mantle is enriched in these elements.

Lanthanum / Ytterbium (La/Yb) and Sm/Yb: These ratios indicate strongly fractionated source of magma (Yaxley 200; Xu et.al 2005; Lai et.al. 2012).

Gd/Yb: This ratio is distinctive indicator of the strong fractionation of magma in the garnet stable zone.

Th/Nb: The RTB basalts have relatively higher Th/Nb (average of 120.541) than those of Mantle. Indicating the enriched mantle source.

Th/Ta: The low concentrations of mantle along with Th/Ta ratio of RTB (average) support minimum contamination by crustal rocks (Safonova et.al. 2008; Lai et.al. 2012).

Nb/Th: As the Rajahmundry Trap Basalts (RTB) characteristically have Nb/Th ratio 12.271 and primitive mantle 5.777 and that of continental crust is 1.1 (Tayler and Mc Lennan 1985; Sun and Mc Donough 1995); (Rollinson 1993) these ratios reflect minimum contamination crustal.

Zr/Hf: The Zr/Hf ratio in basalts is not a single constant value but varies significantly depending on the type of basalts and magmatic processes involved in its formation. The ratio typically varies from 35 to 87. While mid oceanic ridge basalts and continental materials show a chondritic Zr/Hf ratio around 35 to 40. Ocean Island basalts commonly exhibit distinctly higher ratios. The Zr/Hf ratio ranges between 37.808 to 40.264 for RTB flows in all the locations indicates fractional crystallisation, especially the crystallization of Zircon for lowering the ratio

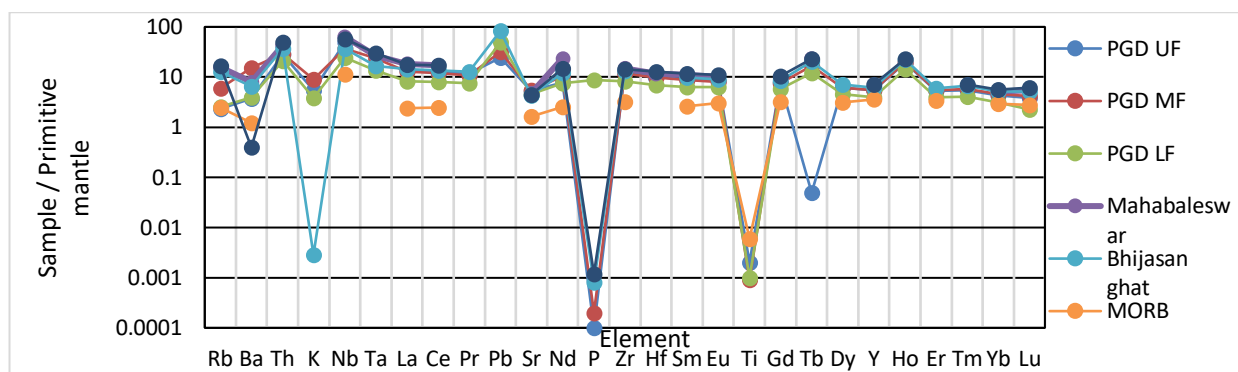


Fig. No: 25. Primitive mantle – normalised trace elements distribution for three flows in Pangidi(PGD) area along with Mahab (Manabaleswar) (K.B. Knight et.al.2003), Bijasanghat (H.C.Sheth et.al), MORB (Shen-SU Sun et.al. 1979) and Kolahapur Unit (Ajoy K Baksi 2001). (after Mc Donough et al.,1995).

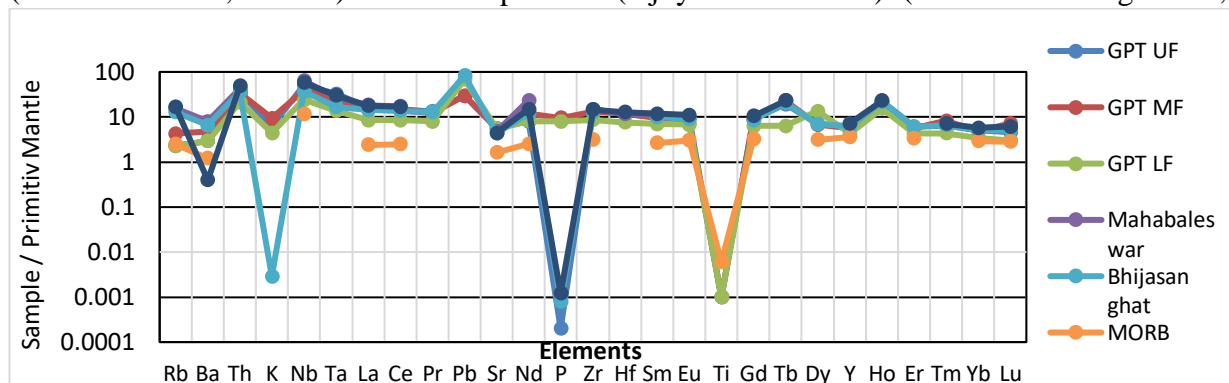


Fig. No: 26. Primitive mantle – normalised trace elements distribution for three flows in Gowripatnam(GPT) area along with Mahab (Manabaleswar) (K.B. Knight et.al.2003), Bijasanghat (H.C.Sheth et.al), MORB (Shen-SU Sun et.al. 1979) and Kolahapur Unit (Ajoy K Baksi 2001) (after Mc Donough et al.,1995).

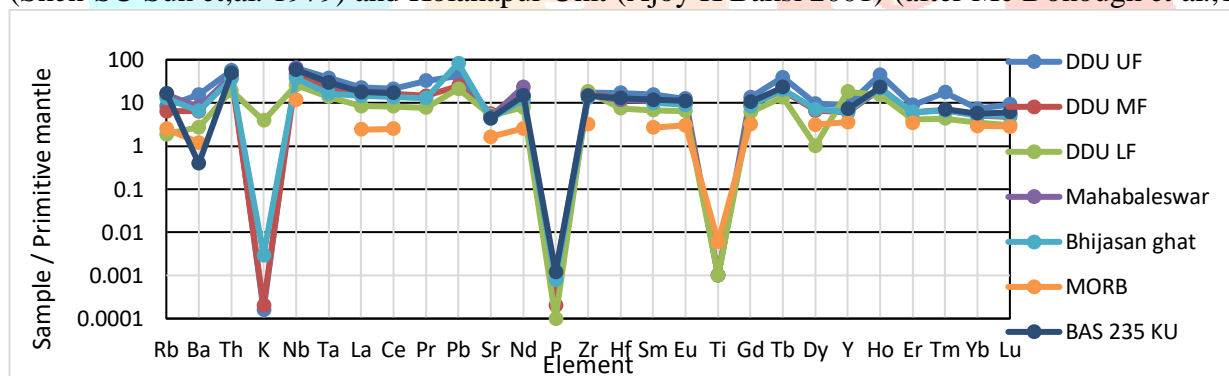


Fig. No: 27. Primitive mantle – normalised trace elements distribution for three flows in Duddukuru(DDU) along with Mahab (Manabaleswar) (K.B. Knight et.al.2003), Bijasanghat (H.C.Sheth et.al), MORB (Shen-SU Sun et.al. 1979) and Kolahapur Unit (Ajoy K Baksi 2001) (after Mc Donough et al.,1995).

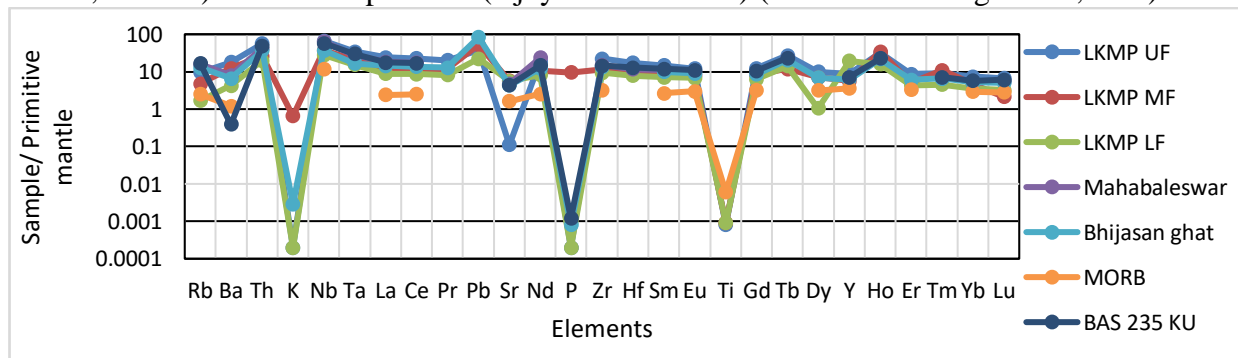


Fig. No:28. Primitive mantle – normalised trace elements distribution of three flows in Lakshmpuram (LKMP) along with Mahab (Manabaleswar) (K.B. Knight et, al.2003), Bijasanghat (H.C.Sheth et.al), MORB (Shen-SU Sun et.al. 1979) and Kolahapur Unit (Ajoy K Baksi 2001) (after Mc Donough et al.,1995).

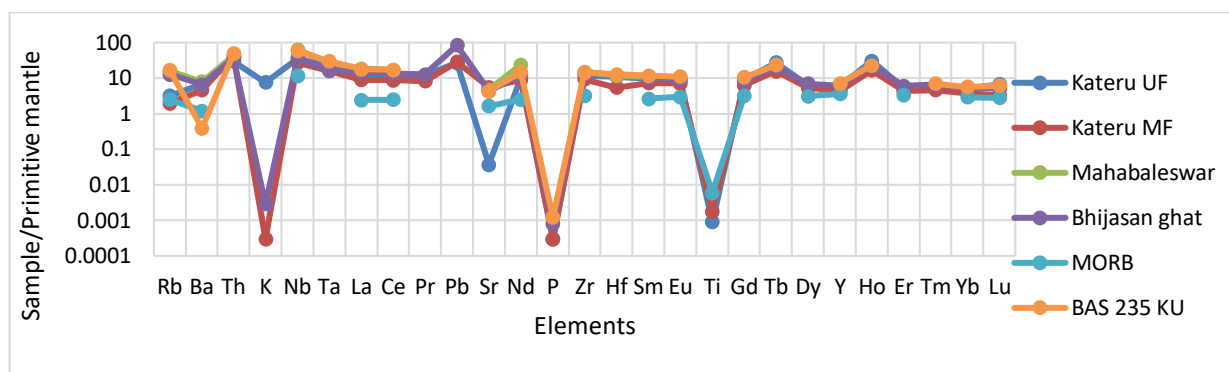


Fig. No:29. Primitive mantle – normalised trace elements distribution of Upper and middle basalts flow in Kateru along with Mahab (Manabaleswar) (K.B. Knight et, al.2003), Bijasanghat (H.C.Sheth et.al), MORB (Shen-SU Sun et.al. 1979) and Kolahapur Unit (Ajjoy K Baksi 2001) (after Mc Donough et al.,1995).

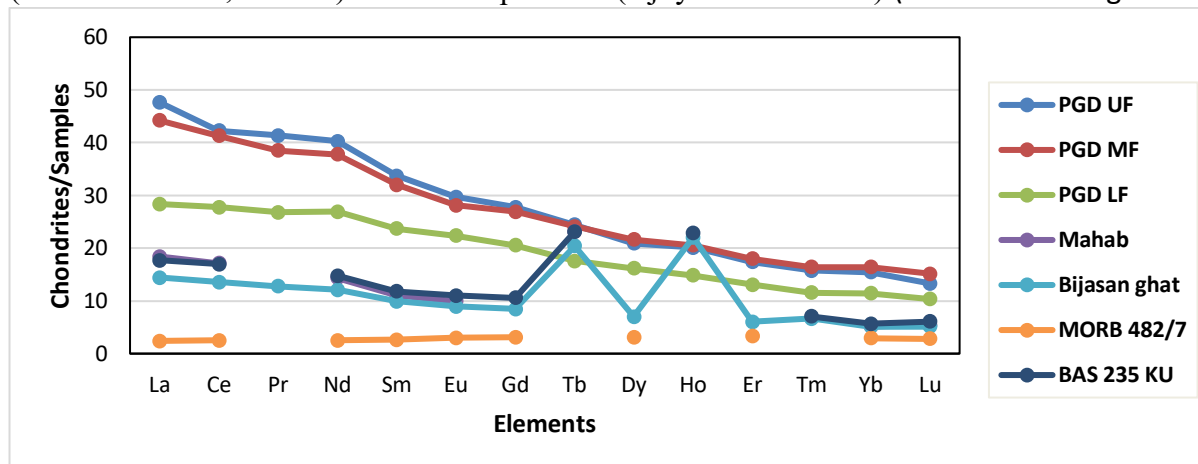


Fig. No: 30. Chondrite Normalized Rare Earth Elements distribution for three basalt flows at Pangidi along with Mahab (Manabaleswar) (K.B. Knight et, al.2003), Bijasanghat (H.C.Sheth et.al), MORB (Shen-SU Sun et.al. 1979) and Kolahapur Unit (Ajjoy K Baksi 2001) (after McDonough and Sun 1995).

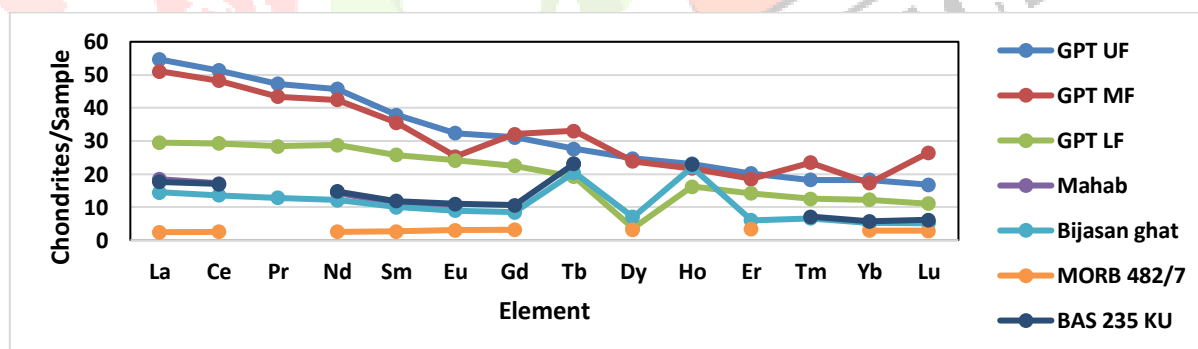


Fig. No: 31. Chondrite Normalized Rare Earth Elements distribution for three basalt flows at Gowripatnam(GPT) along with Mahab (Manabaleswar) (K.B. Knight et.al.2003), Bijasanghat (H.C.Sheth et.al), MORB (Shen-SU Sun et.al.1979) and Kolahapur Unit (Ajjoy K Baksi 2001) (after McDonough and Sun 1995).

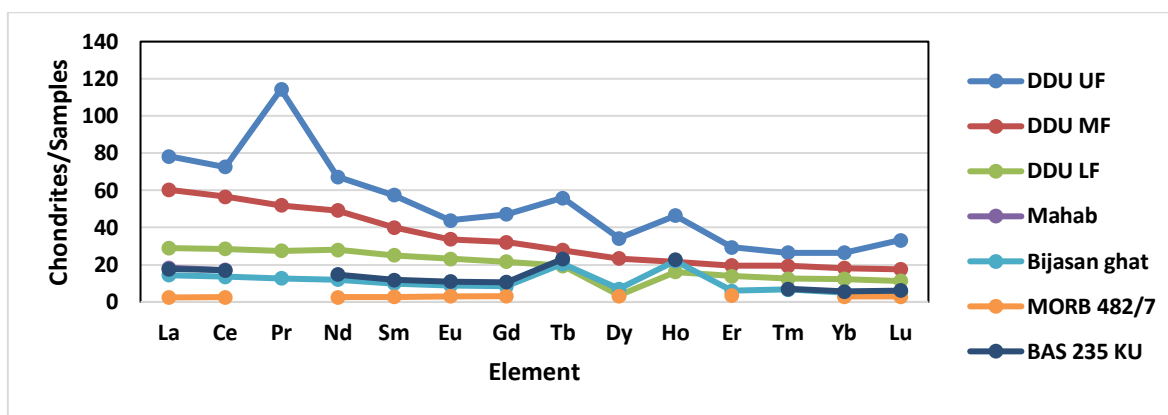


Fig. No: 32. Chondrite Normalized Rare Earth Elements distribution for three basalt flows at Duddukuru (DDU) along with Mahab (Manabaleswar) (K.B. Knight et.al.2003), Bijasanghat (H.C.Sheth et.al), MORB (Shen-SU Sun et.al. 1979) and Kolahapur Unit (Ajoy K Baksi 2001) (after McDonough and Sun 1995).

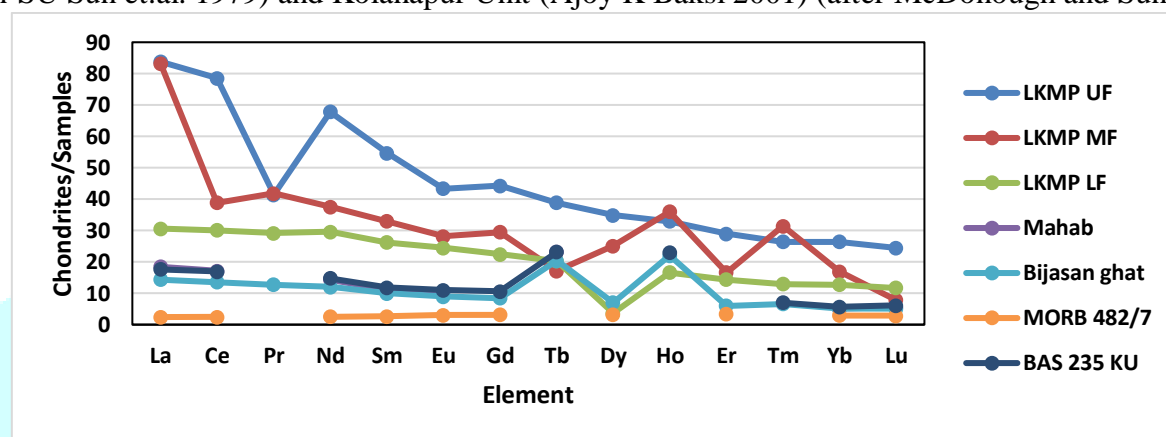


Fig. No: 33. Chondrite Normalized Rare Earth Elements distribution for three basalt flows at Lakshmipuram (LKMP) along with Mahab (Manabaleswar) (K.B. Knight et.al.2003), Bijasanghat (H.C.Sheth et.al), MORB (Shen-SU Sun et.al.1979) and Kolahapur Unit (Ajoy K Baksi 2001) (after McDonough and Sun 1995).

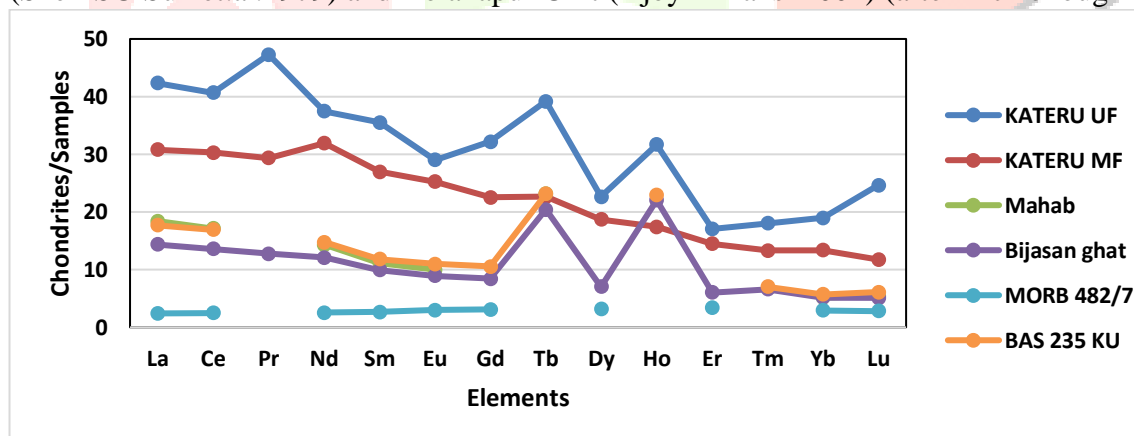


Fig. No: 34. Chondrite Normalized Rare Earth Elements distribution for two basalt flows at Kateru along with Mahab (Manabaleswar) (K.B. Knight et.al.2003), Bijasanghat (H.C.Sheth et.al), MORB (Shen-SU Sun et.al. 1979) and Kolahapur Unit (Ajoy K Baksi 2001) (after McDonough and Sun 1995).

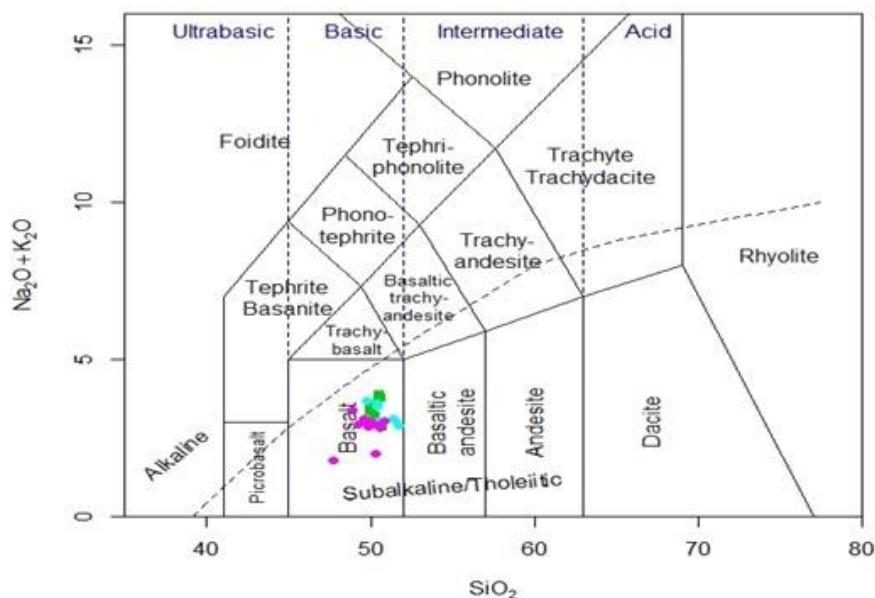


Fig. No.35. Total Alkali vs Silica diagram (after Lebas et.al., 1986 for basalt flows of the study area; Green coloured dots indicate Upper Basalt flow, Light Blue colour dots indicate Middle Basalt flow, and Pinck coloured dots indicate the Lower Basalt flow of the study area.

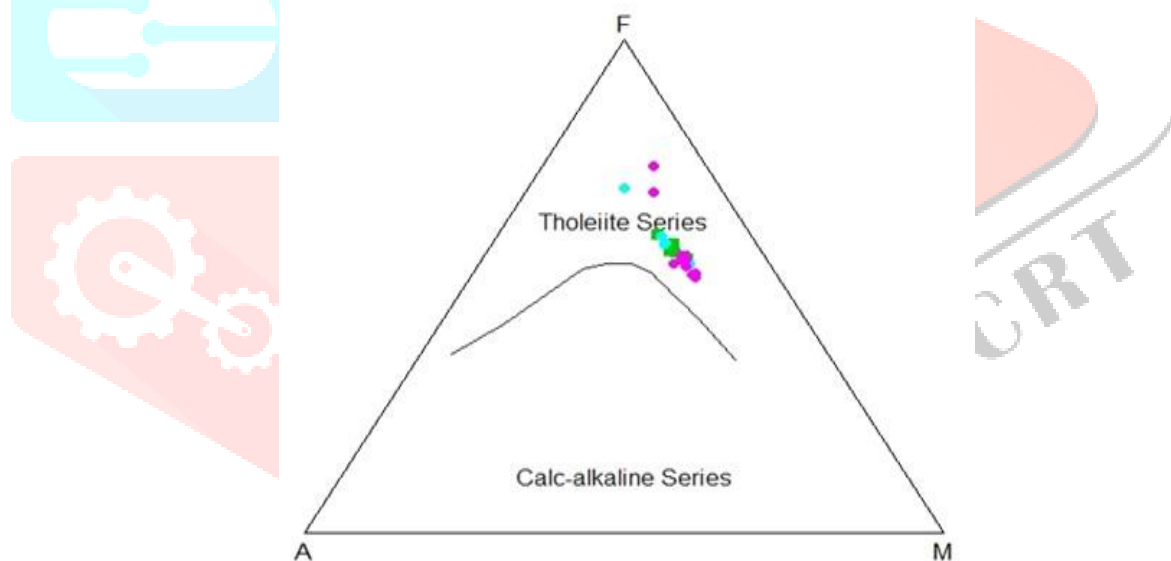


Fig. No.36. AFM plot (after Irvine and Baragar, 1971) for Rajahmundry trap Basalts flows. A- $\text{Na}_2\text{O} + \text{K}_2\text{O}$; F- FeO; M- MgO (Colour coding same as in Fig. 35).

Conclusions:

1. Rajahmundry Trap Basalts depict distinctly tholeiitic character with SiO_2 ranging from 47.5 – 48.06wt% and moderate to high ranges of MgO 2.71 – 8.30wt% and CaO 5.69 – 12.57wt% and Al_2O_3 ranging in between 11.80 and 14.63wt%.
2. The total Alkalis ($\text{K}_2\text{O} + \text{Na}_2\text{O}$) Vs Silica (SiO_2) indicates sub-Alkaline tholeiitic character of these RTB flows.
3. Primitive mantle normalized spider diagrams indicates that source mantle for RTB flows is much depleted in P, K and Ti partially enriched in Rb, Ba, Sr, Nd, Gd, Dy Y, Yb, Yb, Tm, Er, Eu and Lu moderately enriched in Ce, La, Pr, Zr, Tb and highly enriched in Th, Nb, Ta, Ho, Pb.
4. The presence of Normative quartz along with Stishovite and Cristobalite identified in X-ray Powder pattern is sure evidence for deep mantle source for-basaltic magmas probably either lower mantle or transition zone and basalt magma brought up to surface by up-welling convection currents.

5. Trace elements substitute major elements in the lattice structure of minerals and the major and trace elements pairs like Co vs Fe, Ni vs Mg, Mg vs Mu, Fe vs V, Fe vs Co, Fe vs Cr, Al vs Ti, Mg vs Li, Ca vs Sr, K vs Pb, K vs Ba, K vs Rb showed positive relationships whereas some rare earth elements like Pr, Ce, La, Nd, Y, and Gd showed negative relationships with Ca and Sc showed positive relation with Fe.

Acknowledgement

We are very much thankful to Dr. Rammohan Rao Head of Geochemistry division of the National Geophysical Research Institute (NGRI), Hyderabad for great help in chemical analysis of Major, Minor, Trace, and REE analyses. Our sincere thanks to Mr. B Srinivasa Rao Senior Geologist in petrology Division at Geological Survey of India (GSI) Hyderabad for his great support, good suggestions and technical support. And also, we are ever grateful to Mr. N Venkayya senior project Associate APSAC Vijayawada, for his utmost help in the preparation of maps and other technical support.

REFERENCES

1. Amy L. Lewis et al., 2021; Effects of mineralogy, chemistry and physical properties of basalts on carbon capture potential and plant – nutrient element release via enhanced weathering. Applied Geochemistry 132 Elsevier.
2. Arthur Vienne, Silvia Poblador, Miguel Portillo – Estrada, Jens Hartmann, Samuel Ijehon, Peter Wade and Sara Vicca, 2022 Enhanced Weathering Using Basalt Rock Powder: Carbon Sequestration, Co- Benefits and Risks in a Mesocosm Study with Solanum tuberosum. Frontiers; Original Research published 17 May 2022. Volume Article No. 869456.
3. Bakshi A K, Byerly G R, Chan L H and Farrar E 1994 Intracanyon flows in the Deccan Province, India? Case history of the Rajahmundry traps; Geol. 22 605–608.
4. Bakshi A 2001 The Rajahmundry Traps, Andhra Pradesh: Evaluation of their petrogenesis relative to the Deccan traps; Proc. Indian Acad. Sci. 110 397–407.
5. Bakshi A K 1987 Critical evaluation of the age of the Deccan Traps, India: Implications for flood-basalt volcanism and faunal extinctions; Geology 15 147–150.
6. Bakshi A K 1990 The timing and duration of Mesozoic/Tertiary flood basalt volcanism; Eos, Trans. Am. Geophys. Union 71 1835–1840.
7. Bakshi A K 1994 Geochronological studies on whole-rock basalts, Deccan Traps, India: Evaluation of the timing of volcanism relative to the K-T boundary; Earth Planet. Sci. Lett. 121 43–56
8. Bakshi A K 1999 Revolution of plate motion models based on hotspot tracks in the Atlantic and Indian Oceans; J. Geol. 107 13–26.
9. Bakshi A K 2001 Search for a deep mantle component in mafic lavas using a Nb - Y - Zr plot; Can. J. Earth Sci. 38 813–824.
10. Bakshi, A.K. (2001b). The Rajahmundry traps, Andhra Pradesh: evaluation of petrogenesis relation to the Deccan Traps.
11. Balaram, V, and Saxena, V.K. (1988). Determination of Rare earth elements in standard geological reference samples by Inductively Coupled Plasma Mass Spectrometry (ICPMS) using Indium as internal standard. Proc. 1st International Conference on plasma source Mass Spectrometry, Durban, U.K., p.441.
12. Bhimasankaram VLS 1965 Paleomagnetic directions of the Deccan Traps of Rajahmundry, Andhra Pradesh, India; Geophys. J. 9 213–219.
13. Bibhas Sen and A. B. Sabale Vol. 78, Nov. 2011, PP. 457 – 467 Journal Geological Society of India. Flow – types and Lav Emplacement History of Rajahmundry Traps, West of River Godavari, Andhra Pradesh.
14. Cande S C and Kent D V 1992 A new geomagnetic polarity time scale for the Late Cretaceous and Cenozoic; J. Geophys. Res. 97 13,917–13,951.
15. Cox, K.G., 1980. A model for flood basalt volcanism. Journal of Petrology 21, 629e650.
16. Cox K G and Hawkesworth C J 1985 Geochemical stratigraphy of the Deccan Traps at Mahabaleshwar, Western Ghats, India, with implications for open system magmatic Processes; J. Petrol. 26 355–377.
17. Ganguly, S., Ray, J., Koeberl, C., Ntaflou, T., Banerjee, M., 2012. Mineral chemistry of lava flows from Linga area of the Eastern Deccan Volcanic Province, India. Journal of Earth System Science 121, 91e108.

18. Govindan, A., 1981. Foraminifera from the Infra- and Inter-Trappean Subsurface Sediments of Narsapur Well-I and the Age of the 'Deccan' Trap Flows. Indian Colloquium on Microalaeontology and Stratigraphy 9th Proceedings, pp. 81e93.
19. Gowtham Sen, D. Chandrasekharan 2011. Deccan traps flood Basalts province An Evaluation of the Thermochemical plume Model. Springer Science + Business media.
20. G.W.Tyrrell 1926 The principles of Petrology B.I Publications 54, Janapath, New Delhi-11001 published
21. Hughes, C.J., 1982. Igneous Petrology. Elsevier, New York, p. 551. Ionov, D.A., Griffin, W.L., O'Reilly, S.Y., 1997. Volatile-bearing minerals and lithophile trace elements in the upper mantle. Chemical Geology 141, 153e184.
22. Irvine, T.N., Baragar, W.R.A., 1971. A guide to the chemical classification of the common volcanic rocks. Canadian Journal of Earth Science 8, 523e548.
23. I. Safonova, S. Kojima, S. Nakae, R.L. Romer, R. Seltmann, H. Sano, T. Onoue 2015 Oceanic 24. Island basalts in accretionary complexes of SW Japan: Tectonic and petrogenetic implications. Journal of Asian Earth Sciences 113 508-523.
24. I Sabel, M. Fendley, Courtney, J. Sprain, Paul R. Renne 2020 No Cretaceous- Paleogen Boundary in Exposed Rajahmundry traps: A Refined Chronology of the Longest Deccan lava flows from 40Ar/39Ar Daes, Magnetostratigraphic, and Biostratigraphy. American Geophysical Union.
25. Keller, G., Adatte, T., Gardin, S., Bartolini, A., Bajpai, S., 2008. Main Deccan Volcanism phase ends near the K-T boundary: evidence from the Krishna-Godavari Basin, SE India. Earth and Planetary Science Letters 268, 293e311.
26. Krishnan M S 1950 Limestone and ochre near Kovvur and Rajahmundry, Madras Presidency; Geol. Surv. India Record 81 297-314.
27. Lakshminarayana, G., 1995a. Gondwana sedimentation in the Chintalapudi subbasin, Godavari valley, Andhra Pradesh. Journal of Geological Society of India 46, 375e383.
28. Lakshminarayana G, Manikyamba C, Tarun C, Khanna P, Kanakadande P and Raju K 2010 New observations on Rajahmundry Traps of the Krishna-Godavari Basin; J. Geol. Soc. India 75 807-819.
29. Lakshminarayana, G., 1995b. Fluvial to estuarine transitional depositional setting in the Cenozoic Rajahmundry Formation, K-G basin, India. Indian Minerals 49, 163e176.
30. Lakshminarayana, G., 1996. Stratigraphy and Structural Framework of the Gondwana Sediments in the Pranhit-Godavari Valley, Andhra Pradesh. Proceedings of the IXth International Gondwana symposium 1, pp. 311e330.
31. Lai, S., Qin, J., Li, Y., Li, S., Santosh, M., 2012. Permian high Ti/Y basalts from the eastern part of the Emeishan Large Igneous Province, southwestern China: petrogenesis and tectonic implications. Journal of Asian Earth Sciences 47, 216e230.
32. Le Bas, M.J., Le Maitre, R.W., Streckeisen, A., Zanem, B., 1986. A chemical classification of volcanic rocks based on the total alkali-silica diagram. Journal of Petrology 27, 745e750.
33. L. Rama Rao S.R Narayana Rao & K Sripada Rao Feb.1936 On the age of the Deccan traps near Rajahmundry.
34. Manikyamba C, Sohini Ganguly, M.Santhosh, Abhishek Saha, G. Lakshminaryana 2015 Geochemistry and petrogenesis of Rajahmundry trap basalts of Krishna-Godavari Basin, India. Elsevier Geoscience Frontiers 6 (2015) 437-451.
35. Malarkodi N, G. Keller, P.J. Fayazudeen and U.B. Mallikarjuna 2010 Foraminifera from the Early Danian Intertrappean Beds in Rajahmundry Quarries, Andhra Pradesh. Journal Geological Society of India. Vol. 75, pp. 851-863.
36. Mc Donough, W.F. and Sun, S. S.: The Composition of the Earth, Chem. Geol., 120, 223-254, 1995.
37. Potwardhan, A.M. 2010. The Dynamic Earth System. Second Edition, PHI Liowring Pvt.Ltd.
38. Raju D S N, Rao C N and Sengupta B K 1965 Paleocurrents in Miocene Rajahmundry formation, Andhra Pradesh, India; J. Sedim. Petrol. 35 758-762.
39. Rao A T, Srinivasa Rao K and Vijaya Kumar V 2002 Basic volcanism along K-boundary from Rajahmundry, east coast of India; J. Geol. Soc. India 60 583-586.
40. Rollinson, H.R., 1993. Using Geochemical Data: Evaluation, Presentation, Interpretation. John Wiley, Chichester, 352pp.
41. Self S, Jay A E, Widdowson M and Kaszthelyi L P 2008 Corelation of the Deccan and Rajahmundry trap lavas: Are these the longest and largest lava flows on Earth? J. Vol. Res. 172 3-19.
42. Sen G 1986 Mineralogy and petrogenesis of the Deccan Trap flows around Mahabaleswar; J. Petrol. 27 627-663.

43. Sen, G., 1988. Possible depth of origin of primary Deccan tholeiitic magma. Geological Society of India Memoir 10, 34e51.
44. Sen, B., Sabale, A.B., 2011. Flow-types and lava emplacement history of RTB, west of river Godavari, Andhra Pradesh. Journal of Geological Society of India 78, 457e467.
45. Sethna S F, Czygan W and Sethna B S 1987 Iron–titanium oxide geothermometry for some Deccan Trap tholeiitic basalts, India; J. Geol. Soc. India 29 483–488.
46. Sun, S.S., McDonough, W.F., 1989. Chemical and isotopic systematics of oceanic basalts: implications for mantle composition and processes. In: Saunders, A.D., Norry, M.J. (Eds.), Magmatism in Ocean Basins. Geological Society of London Special Publication 42, pp. 313e345.
47. Taylor S R and McClelland S M 1985 The continental crust: its composition and evolution; (Oxford: Blackwell) 312pp.
48. Wilson, M., 1989. Igneous Petrogenesis. Unwin Hyman, London, p. 466.

